Buffer modification: A case study with polystyrene beads, DU145-, and MCF7 cell lines

by Olivia Rengbrandt

Master's Thesis in
Biomedical Engineering

LUND
UNIVERSITY

Faculty of Engineering LTH
Department of Biomedical Engineering

Supervisor: Dr. Thierry Baasch
Co-supervisor: Dr. Andreas Lenshof
Examiner: Pr. Thomas Laurell

June, 2023

Abstract

Separation of cancer cells gives advantages in understanding the disease, guiding treatment decisions, and facilitating drug development. Overall, separation plays an important role in biological research. Acoustophoresis is a technique that utilizes acoustic waves to separate particles and cells suspended in a buffer medium. The efficiency of this separation process depends on the relative acoustic mobility of the cells and particles compared to the buffer medium. Factors such as density, size, and compressibility determine the mobility ratio, with a higher ratio indicating better separation. In this thesis, the mobility ratios between the particles and cells targeted for separation were evaluated, with the goal to select the optimal buffer medium that yields the highest separation. Polystyrene beads, DU145 prostate cancer cells, and MCF7 breast cancer cells were used for the experiments. By optimizing the buffer medium, the acoustic mobility of the particles and cells was modified. One of the findings was that the most effective buffer medium for separating polystyrene beads in varying sizes was determined to be 20% Iodixanol, highlighting differences in material properties between the beads. For DU145 cells, the addition of Iodixanol to the buffer resulted in optimal separation from the polystyrene beads. Except in the case of 4.99 μm beads, where PBS proved to be the optimal buffer medium. For MCF7 cells, a sign change for the acoustic contrast factor was obtained when adding 10% and 20% Iodixanol to the buffer, indicating optimal separation. With this knowledge, the behaviour of these cell lines are clearer and future research can be made in order to obtain separation between these cells and other cells.

Popular science article

Separation of cancer cells is used in biological research and is an important tool in understanding the disease. Separation of one cell type from another can be obtained by using acoustophoresis - a process that utilizes sound waves in a microfluidic chip. Acoustophoresis has proven to be highly advantageous in the fields of biological research and disease diagnostics. Its benefits include the requirement of only small sample volumes, making it a cost-effective technique. Moreover, acoustophoresis maintains the viability of the cells that are separated. Presently, acoustofluidic devices enable the separation of lymphocytes from granulocytes, as well as the isolation of white blood cells from platelets, among other applications involving the manipulation of small cell samples. To make the separation work, transducers are placed on the channel wall of the microfluidic chip. This will apply an acoustic standing wave field to the main flow channel. Depending on the properties of the cells, such as size, density and compressibility, the cells move in different speeds. The half wavelength resonance applied will make faster cells migrate to the center of the channel and slower will migrate to the sides of the channel. This will lead to separation of particles with different properties. In this thesis, different buffer mediums were used in order to enhance separation between two different cell lines and polystyrene beads. The aim is to gain a deeper knowledge in how the cells behave in the different buffers and if it is possible to separate them from beads. With this knowledge, future research can be made in order to obtain separation between these cell lines and other cells. This in turn would help biological research and disease diagnostics forward. Furthermore, this thesis aims to explore the behaviour for polystyrene beads in varying sizes and in different buffers. Their behaviour is of importance in research, since they are commonly used. To determine how well the separation was, the mobility ratios between the cells and beads were calculated. In other words,the displacement of particles and cells from their initial position in the chip was measured. A higher mobility ratio would indicate better separation.

The thesis utilized polystyrene beads in different sizes that were separated from each other using two different buffers: MQ water and 20% Iodixanol. Moreover, two cell lines were used: DU145, a prostate cancer cell line, and MCF7, a breast cancer cell line. These cancer types are among the most common in modern times and were obtained from humans and cultivated in a suitable laboratory setting to obtain an sufficient quantity of cells for experimentation. Three different buffer media were tested for the cells: phosphate-buffered saline (PBS) and two concentrations (10% and 20%) of Iodixanol. It was observed that, in general, the separation of DU145 and MCF7 cells was most effective when Iodixanol was added to the buffer medium. Particularly for MCF7, the addition of Iodixanol change the sign of the acoustic contrast factor of the cells, causing them to no longer migrate towards the central outlet, thereby enhancing separation. Another interesting finding appeared from the experiments involving only polystyrene beads, where a higher mobility ratio was achieved in 20% Iodixanol compared to MQ water. This suggests that the polystyrene beads have distinct material properties despite sharing the same composition. This unexpected outcome should

be investigated further.

Throughout the experiments, different challenges were encountered. Fibers were found inside the chip that hindered its proper utilization. Furthermore, changing and tuning the total flow rate became a problem. Attempts were made to clean the chip multiple times to get rid of the fiber, but without satisfactory outcome. As a result, a few experiments had to be run with fibers present in the chip due to the limited availability of cells. However, a test run was also performed using polystyrene beads in the presence of the same fiber to assess the potential impact on the results. Fortunately, the fiber did not affect the outcomes. The issue with flow rate calibration was resolved by adjusting it gradually rather than making sudden changes. Consequently, all experiments took longer than expected, limiting the ability to test as many buffers as initially planned. Furthermore, working with cells proved to be more challenging than expected. One can sometimes forget that they are living creatures and needs to be treated as such.

The conclusion that can be drawn from this thesis is that in general, adding Iodixanol to the buffer gives a better separation for DU145 and MCF7 cells, as well as for polystyrene beads. This knowledge can give a deeper understanding in cancer biology with a future goal to separate these cancer cells from other cell lines. However, further research needs to be done regarding the material properties of the beads. As MCF7 has negative contrast factor when adding Iodixanol up to 20%, they would be possible to separate from DU145 in that specific buffer. However, it would also be interesting to test this hypothesis since we know that science does not always give the intended outcome.

Acknowledgements

First of all, I would like to thank Thomas Laurell for letting me start this project, and for believing in me even if I did not have very much experience in the field. I am incredibly grateful for this opportunity and the assistance I received along the way. Despite facing various challenges during my project, I was fortunate to have received valuable support that helped me overcome these obstacles. Even when I felt alone, I realized I had a supportive group of individuals who helped me and offered their assistance and encouragement. Thierry Baasch, thank you for always being there to answer my questions and guide me through the thesis and the difficult MATLAB codes. Thank you for always making me comfortable asking any question without hesitation. Andreas Lenshof, thank you for your invaluable presence and assistance in the lab. Despite all the troubles I encountered, you always came with a positive attitude and could even make me laugh in the most frustrated situations. Thank you for your exceptional care you provided to my cells when life came in the way. Cecilia Magnusson, thank you for your guidance and insights on working with cells. Your willingness to share your expertise and provide guidance during the process was truly appreciated. Linda Péroux, I want to express my gratitude for promptly addressing my questions and emails regarding your thesis. Lovisa Silversand, thank you for starting this project with me. Even if it did not end the way we thought, I am grateful for the initial journey we shared and the experiences we had together. I would also like to extend my thanks to everyone else in the biomedical building for their kindness, assistance, and willingness to lend a helping hand whenever needed. Last but not least, I would like to thank Jonathan Vaknine and the rest of my friends and family for supporting me throughout this journey. It has been a rocky road, but you have always been there for me.

Notations and symbols

Symbol	Description
Re	Reynolds number
μ	Viscosity of fluid
u	Average flow speed of fluid
p_1	First order of pressure field p_a
k	Wavenumber
ϕ	Acoustic contrast factor
ϕ_1/ϕ_2	Acoustic contrast factor for particle 1 devided with particle2
ρ_p	Density of the particle
ρ_m	Density of the medium
κ_p	Compressibility of the particle
κ_m	Compressibility of the medium
$\vec{F}_{rad}$	Radiation force
$\vec{F}_{drag}$	Stokes drag force
a	Radius of the particle/cell
E_{ac}	Acoustic energy density
Q_{tot}	Total flow rate
Q_{in}	Inlet flow rate
Q_{out}	Outlet flow rate
r_{in}	Inlet splitting ratio
r_{out}	Outlet splitting ratio
η	Dynamic viscosity of the fluid
$v_{p(y)}$	Particle velocity in y-direction
$MR_{1,2}$	Mobility ratio of particle 1 over particle 2

Contents

CHAPTER 1

Introduction

The objective of this chapter is to provide a comprehensive background and outline the aims of the thesis.

Acoustophoresis is a microfluidic method that utilizes ultrasound in order to move cells and particles in an acoustophoretic chip [1]. In this chip, particles suspended in a buffer medium are affected by an acoustic radiation force when exposed to an acoustic standing wave field [2]. The half wavelength resonance affects particles to move either to the pressure node of the channel located in the center of the acoustophoretic chip, or to the antinode located on the sides of the acoustophoretic chip [2]. As a result, the particles can exit the chip through different outlets, leading to separation. The force acting on the particles depends on particles properties such as density, size and compressibility [1]. This enables manipulation of cells and particles on the micro scale [3][4].

In acoustic separation, the buffer conditions used are important. Since the acoustic mobility of cells depends on the buffer medium [5], the medium can be modified and optimized in order to obtain better separation of cells in a sample. For example, some sub populations of cells have similar acoustic mobility conditions in water that hinders an efficient separation. The selection of a buffer can be examined by studying the mobility ratio between particles. According to Urbansky et al, [3] modifications in the properties of the medium can impact the separation. Typically, particles denser than the suspending medium exhibit a positive acoustic contrast factor. The sign on the contrast factor cause the particles to migrate towards the pressure node or the antinode within the acoustic field. However, when the density of the medium is increased and its compressibility is decreased, the acoustic contrast factor of the cell decreases. As a result, the acoustophoretic mobility of the cell is reduced. By achieving a negative acoustic contrast factor, the cell can be directed towards the pressure antinode, facilitating movement in that direction [3].

There are many biological applications for acoustophoresis, such as isolate circulation tumor cells from blood or separate different leukocyte subpopulations from each other [6] [7]. Improved separation of cells or specific substances from a mixture is of great advantage in biological research and disease diagnostics, since other cells or substances in the mixture can contribute to incorrect data [8]. Separation efficiency and purity can be examined by labelling the cells and use flow cytometry [6]. Acoustophoresis is a label-free technique and the requirement of only small sample volumes make it cost effective [5]. It is also a method that is easy to use. Furthermore, it preserves the viability of the separated cells [3].

This thesis will utilize two different cancer cell lines together with polystyrene beads. The

buffer medium is modified to evaluate the acoustic properties of the cells. The effectiveness of the separation process is determined by calculating the mobility ratios between the cancer cells and the particles. A higher mobility ratio would indicate better separation. Acoustophoresis is used throughout the experiments to investigate the behavior of the cancer cells. This knowledge is valuable for future studies and gives a start to research the possibility to separate these cancer cells from other cell types, and what buffer to use in order to do so. In other words, experiments with cells with polystyrene beads can provide initial insights and help optimize experimental parameters in order to have a possibility to separate these cancer cells from other cell types in a blood sample in the future. This would in turn help cancer research and disease diagnostics forward. Currently, the optimal buffer for effectively separating these cancer cells has not been identified. The use of polystyrene beads allows for easier evaluation of the results with cancer cells, as the behaviour of the beads is well known in research. Furthermore, polystyrene beads are easy to use and does not need delicate handling as cells do.

1.1. Thesis aims

This thesis aims to explore the potential of altering and optimizing buffer mediums and thereby the ratio of the acoustic mobility for two distinct cell lines - DU145, a prostate cancer cell line, and MCF7, a breast cancer cell line - with polystyrene particles in different sizes. By doing so, it is hypothesized that the acoustic mobility ratio can be modified, potentially leading to improved separation capabilities between polystyrene particles and cells. This thesis also aims to evaluate if the flow measurement of the mobility ratio can be used to optimize the buffer.
Experiments using only polystyrene particles in different sizes and in different buffers should also be evaluated in order to explore their separation. This will give valuable knowledge about the behaviour of polystyrene beads and their material properties. This is important since polystyrene beads are often used as reference beads in research.

To sum up, the overall goals of this thesis are to:

- Enhance the separation between two different cancer cell lines and polystyrene beads by modifying the buffer medium and thereby evaluate the behaviour of the cancer cells in the different buffers
- Evaluate separation between polystyrene beads of different sizes

CHAPTER 2

Theory

The objectives of this chapter are to provide an understanding of the principles behind acoustophoresis. It will also illustrate the setup employed in this thesis and explain how to optimize a buffer connected to the setup.

2.1. Acoustophoresis

The fluid flow within the channel of an acoustophoresis chip displays laminar flow which is characterized by smooth and predictable flow lines within the channel. Laminar flow is necessary for enabling the simultaneous movement of two or more fluids in a microchannel without interference. This is due to the simplicity with which laminar flow can be modeled. It is also due to its predictability. Laminar flow occurs at low Reynolds numbers, where the fluid flows in distinct layers. Usually, acoustophoretic separation occurs at low Reynolds number [9].

The Reynolds number is defined as the ratio of inertial to viscous effects in a channel flow:

$$Re = \frac{\rho u L}{\mu} \tag{2.1}$$

with ρ being the density of the fluid, u the characteristic flow speed, L the characteristic linear dimension and μ the kinematic viscosity of the fluid. With a Reynolds number smaller than one, hence a very low number, the inertial forces are negligible compared to the viscous forces [10].

By having two acoustic waves with the same frequency and amplitude but with the opposite direction of propagation, one can obtain the acoustic standing waves by superimposing these two acoustic waves. Furthermore, channel resonance is used in order to construct an acoustic field that results in lateral forces. The pressure field can be expressed as following:

$$p_1 = p_a \cdot cos(ky) \tag{2.2}$$

with p_a being the amplitude of the first order pressure field, $k = 2\pi\lambda$ the wave number and y the position of the particle. This is the expression used for one dimension. The radiation

force induced by the acoustic field will move the particle to the pressure node or to the anti-node. What direction the particle will move depends on size, density and compressibility of the particle compared to the buffer medium. A particle with a positive contrast factor will migrate to the pressure node, and a particle with a negative contrast factor will migrate to the pressure antinode [11].

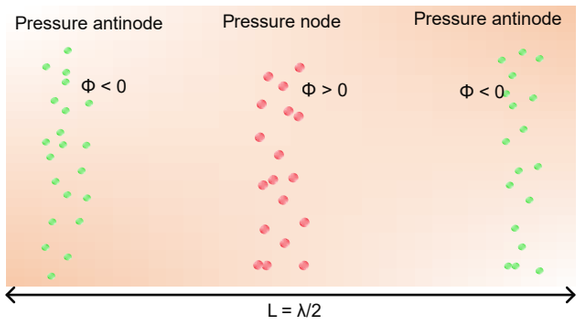

Figure 2.1.: Channel cross section with an acoustic standing wave. Towards the pressure node in the center of the channel, particles with a positive contrast factor will migrate. Particles with a negative contrast factor migrate to the antinodes

The acoustic contrast factor can be described as following:

$$\phi = \frac{5\rho_p - 2\rho_m}{2\rho_p - \rho_m} - \frac{\kappa_p}{\kappa_m} \tag{2.3}$$

with ρ_p being the density of the particle, ρ_m the density of the medium, κ_p the compressibility of the particle and κ_m the compressibility of the medium. The difference in contrast factor between particles or difference in size will lead to a difference in radiation force. The radiation force can be described as following:

$$\vec{F}_{rad} = -4\pi\phi k a^3 E_{ac} sin(2ky) \tag{2.4}$$

with a being the radius of the particle and ϕ the acoustic contrast factor. The difference in the radiation force will make up for the separation of particles. E_{ac} is the acoustic energy density and is described as:

$$E_{ac} = \frac{p_a^2}{4\rho_m c^2} \tag{2.5}$$

where ρ_m is the density of the medium and c the speed of sound in medium.

In figure 2.2, a sketch on the chip looking from above, of the particles in the pre-focusing channel is presented. In figure 2.3, a sketch on the chip looking from above, of the particles in the main channel is presented. The figures show how the particles of different sizes behave in the microfluidic chip.

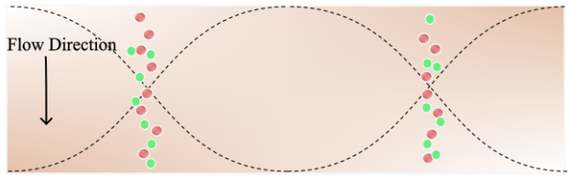

Figure 2.2.: Sketch on the chip looking from above of the prefocusing channel, with two particles with different sizes prefocused in two streamlines. The acoustic standing wave has the wavelength of the channel width

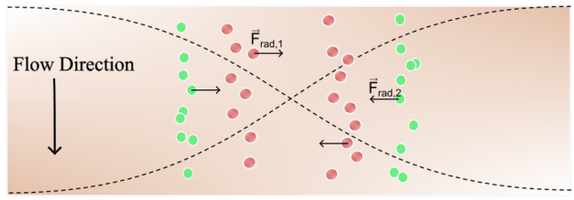

Figure 2.3.: Sketch on the chip looking from above of the main channel with the bigger particles (red), being affected by a higher radiation force than the smaller particles (green). Hence, red ones travel faster towards the the center of the channel which in turn leads to separation of the particles. The acoustic standing wave having the wavelength equal to two times the channel width

2.1.1. The set up

The acoustophoretic chip used in this thesis has a main channel being 375 μm and the prefocusing channel 300 μm. A general setup of the acoustophoretic chip is shown 2.7 and the working set up used in this thesis is showed in 2.4 and is illustrated in 2.5. A sample enters the side inlet of the acoustophoresis chip and the buffer enters through the center inlet. The particles will exit through the side outlet or the center outlet, depending on the acoustic mobility of the particles.

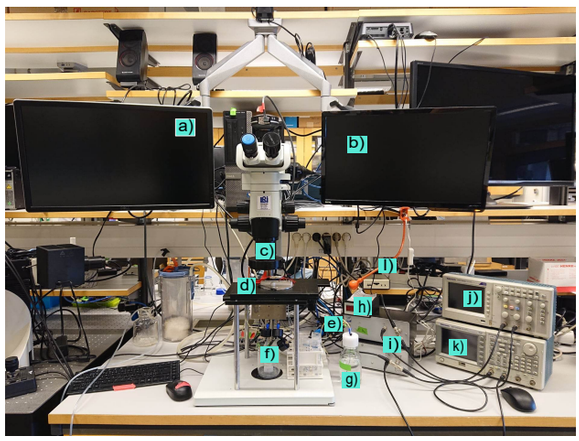

Figure 2.4.: Figure of the set-up that was used for all the experiments in this thesis. a) Camera b) Flow control c) Microscope d) Acoustophoresis chip used during all experiments e) Pressure driven system f) Tubes for sample inlet, center outlet and side outlet g) Buffer h) Temperature control i) Amplifiers j) Oscilloscope k) Signal transducer l) lamp to enhance the picture from the camera

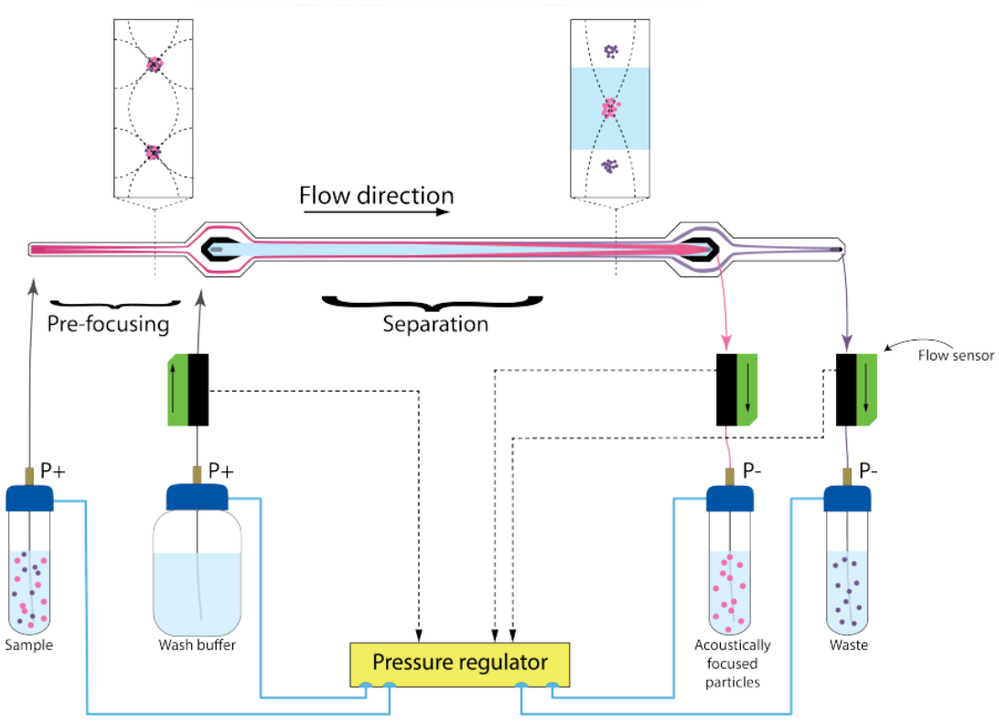

Figure 2.5.: Schematic figure of the acoustophoresis set up. The sample enters through the side inlet and the buffer enters through the center inlet. The sample is pre-focused in the pre-focusing channel. In the main channel, the sample is separated and the acoustically focused particles exit in the center outlet. The wash buffer is changed according to what should be tested. Figure taken from [11]

In order to achieve a more efficient separation a pre-focusing channel is used. The pre-focusing channel has a resonance frequency that differs from the resonance frequency of the main channel. The pre-focusing channel has a resonance frequency around 5 MHz and the main channel around 2 MHz, see figure 2.6. When particles enter the pre-focusing channel, they are pre-aligned using a 5 MHz transducer. This transducer focus the particles in two lines - height and width, into two parallel bands. This is done by generating an acoustic pressure node from top to bottom as well as a double node across the width of the channel. When the particles enter the main channel, close to the channel wall, they will have the same starting position that will result in a better separation. The 2 MHz transducer in the main channel creates an acoustic standing wave field. A pressure node will be situated in the middle of the channel. The particles will now move depending on their acoustophysical properties [3]. See figure 2.5 for cross-section of the pre-focusing and main focusing of particles.

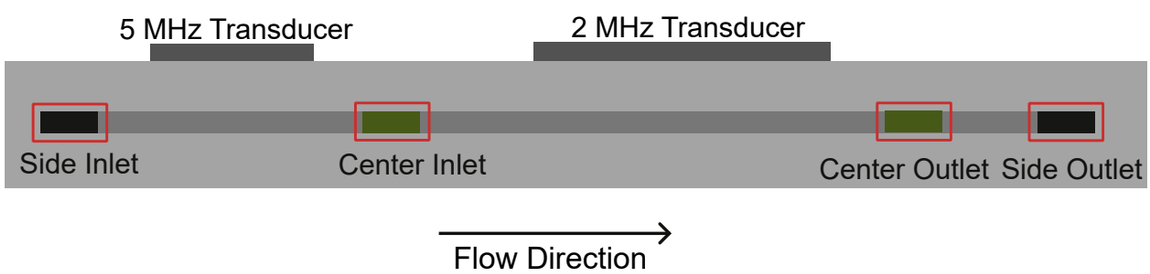

Figure 2.6.: Drawing of the acoustophoresis chip, with the side inlet to the left and side outlet to the right (hence the flow in the chip going from left to right)

The total flow rate in the main channel can be described with following equation:

$$Q_{tot} = Q_{s,in} + Q_{c,in} = Q_{s,out} + Q_{c,out} \tag{2.6}$$

where Q_{tot} is the total flow rate, $Q_{s,in}$ is the flow rate in the side inlet, $Q_{c,in}$ is the flow rate in the center inlet, $Q_{s,out}$ is the flow rate in the side outlet and $Q_{c,out}$ is the flow rate in the center outlet. When the flow rate in the system changes the migration of the particles will change. If the flow rate decreases the particles will have longer time to migrate and the separation will be better.

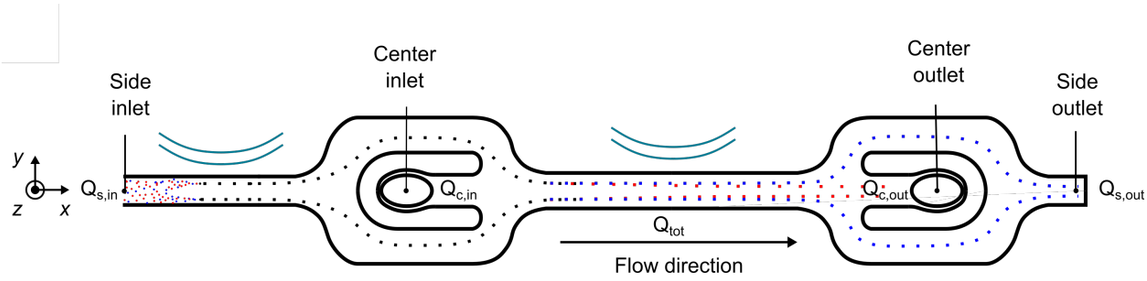

Figure 2.7.: Drawing of the acoustophoretic chip, with the side inlet to the left where the sample enters and side outlet to the right where particles with the lowest acoustic mobility (here; blue) exits. The buffer enters through the center inlet and the particles with the highest acoustic mobility (here; red) exits through the center outlet. The pre-focusing piezo to the left and main focusing piezo to the right. The flow goes from left to right

The inlet splitting ratio is described as:

$$r_{in} = \frac{Q_{s,in}}{Q_{tot}} \tag{2.7}$$

and the outlet splitting ratio can be described as:

$$r_{out} = \frac{Q_{s,out}}{Q_{tot}} \tag{2.8}$$

2.1.2. Buffer optimization

Buffer optimization is a process used in acoustophoresis to enhance the efficiency and selectivity of particle manipulation. The goal is to modify the properties of the buffer solution in order to get an optimized response of the cells/particles that are supposed to be manipulated. If modifying the buffer solution, density and compressibility can be influenced. The density of the buffer solution affect the acoustic radiation force on the particles [3][12].One can thereby affect the acoustic contrast factor of particles and cells by modifying the buffer. Obtaining particles and cells with different signs on the acoustic contrast factors would yield optimal separation.

In this thesis, phosphate-buffered saline (PBS), 10% and 20% Iodixanol are used as buffers. The Iodixanol-containing buffers are prepared using Optiprep, which is a density medium with a concentration of 60% w/v and a density of 1.320 ± 0.001 g/ml. Optiprep is utilized to adjust the density of the buffer medium. To achieve the desired density, Optiprep is diluted with a buffer solution, specifically PBS (10x phosphate-buffered saline). PBS is chosen due to its comparable ionic strength to the cytoplasm of mammalian cells, making it an appropriate choice for maintaining cellular integrity. Moreover, PBS serves as a balanced salt solution, providing a suitable environment for experimental conditions. To make these buffers, 10% Iodixanol are prepared with 16.67 mL 60% w/v Optiprep, 10 mL of 10x PBS and 73.33 mL MQ water. The buffer containing 20% Iodixanol are prepared with 33.33 mL 60% w/v Optiprep, 6.67 mL of 10x PBS and 60 mL MQ water.

The acoustic contrast factor depends on both the properties of the particles and the buffer, see equation 2.3. However, the optimal buffer will depend on the cell and the wanted outcome of the experiment. Overall, buffer optimization is an important tool for optimizing the performance of acoustophoretic systems, and can lead to improvements in particle manipulation efficiency and selectivity.

CHAPTER 3

Background regarding cell lines

The main objectives of this chapter is to give a background regarding the cell lines used in this thesis - DU145 and MCF7.

3.1. Prostate cancer and breast cancer

Aged or impaired cells undergo programmed cell death, allowing for the replacement with fresh cells. Cancer on the other hand is defined by the uncontrolled proliferation of cells that have evaded the natural regulatory mechanisms within the body. Traditionally, cancers are classified based on the organ or tissue from which they originate. However, considering molecular characteristics specific to the cancer cells themselves has become more important in the classification process [13].

Disruptions can occur within this well-regulated process, leading to the proliferation of abnormal or damaged cells. Consequently, the formation of tissue masses known as tumors may transpire. Tumors can be categorized as either cancerous (malignant) or non-cancerous (benign) [14].

In 2018, cancer emerged as the second most prominent cause of mortality worldwide, contributing to approximately 9.6 million deaths, representing one in six recorded fatalities [15].

The two cancer cell lines used in this thesis are DU145 and MCF7. DU145 cell line is a prostate cancer cell line isolated from humans and are about 20 μm in diameter [16]. The cell line has epithelial morphology expressing a polygonal shape. Prostate cancer is the most common cancer disease that affects men. In the early stage, most prostate cancer cells grow slow and as long as the cancer is limited to the prostate gland the symptoms are usually weak [17]. MCF7 cell line are epithelial cells isolated from the breast tissue from humans. They are about 20-30 μm in diameter. Breast cancer is one of the most common type of cancer for women [18].

3.1.1. Cell culturing

DU145 cell line and MCF7 cell line are grown in the cell laboratory due to the standard process of cell culturing. The cells are cultivated in a cell medium with suitable nutrients

combined with anti fungi and antibiotics. As this prevents the cells from getting infected by fungi, bacteria or other microorganisms, this will strengthen the growing process of the cells.

The cell growth medium is changed regularly during the week and cell splitting is done once or twice a week. The cell splitting is done in order to have a balanced amount of growing cells in the flask.

Cell splitting is a procedure in which the cultivated cells in a flask are transferred and divided into smaller portions, that are then transferred to new flasks. This process involves the use of trypsin, PBS, and cell growth medium. Trypsin acts as a proteolytic enzyme, facilitating the detachment of adherent cells from the flask's surface. PBS is employed to neutralize the effects of trypsin, allowing the cells to be split and transferred to new flasks containing fresh cell culture medium.

When cells are required for experiments, they are transferred from the flask onto petri dishes and cultivated for several days to allow them to grow to a suitable quantity, as shown in figure 3.1. Following cultivation, the grown cells are centrifuged to obtain a cell pellet containing only cells. To visualize the cells during the experiment, they are stained with fluorophore-conjugated antibodies. A small quantity of these antibodies is added to the cell solution and incubated for 25 minutes before being ready for use in the experiment.

All medium used when working with cells are heated to 37°C before usage and the cells are kept at 37°C in an atmosphere of 95% air and 5% CO_2.

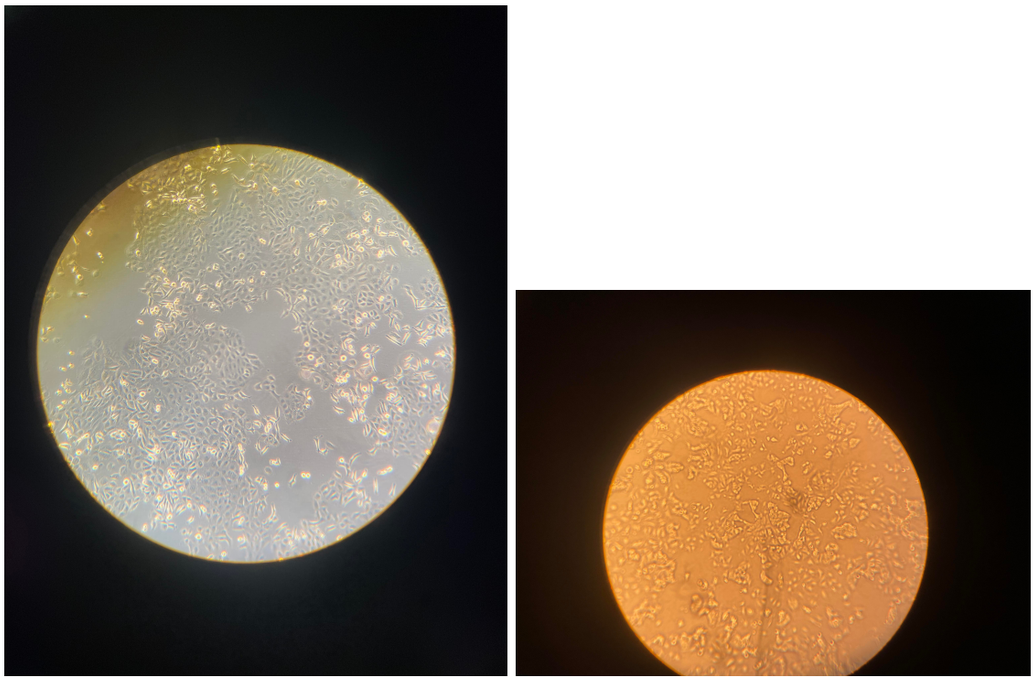

(a) (b)

Figure 3.1.: The appearance of DU145 cells and MCF7 cells growing on petri-dishes in growth medium, for experiments. a) DU145 cells growing on a petri-dish. b) MCF7 cells growing on a petri-dish

The cells in this thesis are stained with two different types of fluorophores to assess which staining appears more pronounced through the camera: calcein AM or EPCAM. The staining with calcein AM was found to be superior and is used in all the experiments. Calcein AM, also known as calcein acetoxymethyl ester, is a cell-permeant dye. Following intracellular esterase-mediated hydrolysis of the acetoxymethyl ester, the initially non-fluorescent calcein AM undergoes conversion into its fluorescent counterpart, calcein [19].

PBS is used when working with cells since cells will disintegrate if suspended in water due to the osmotic pressure difference [20]. The cells are kept on ice when not being used for experiments to slow down metabolic processes and maintain cell viability [21].

3.1.2. Concentration of cells using FACS

The concentration of cells used for each experiment is different every time. It is possible to use Fluorescence Activated Cell Sorting, FACS, to evaluate the concentration. However, this needs to be done for each and every experiment as the concentration differs. In this thesis, it was not possible to do that for every experiment since there was limited amount of cells to work with and all of them were used during one experiment.

A single FACS test was conducted on an MCF7 experiment to obtain a preliminary assessment of the cell concentration for at least one experiment. Initially, a sample consisting of 20 μL of cells was prepared by suspending them in 1 mL of PBS buffer solution and subsequently stained with calcein AM. The flow cytometer was set up for analysis, and the sample was introduced. As the cells passes individually through the laser beam in the set up, they scatter a portion of the laser light. The attached fluorochromes emit fluorescence, which is captured by the detectors within the flow cytometer. The flow cytometer record the emitted fluorescence, as well as forward scatter (indicative of cell size) and side scatter (reflecting cell complexity/granularity) [22].

In figure 3.2a, the live cells are gated as P1. The rest is most likely dead cells or cell debris. The gated cells are plotted in figure 3.2b where the staining is plotted as a function of cell count. Please note that the name of the staining in this plot does not correspond to the flourescent dye used in the experiments, calcein AM. However, Alexa Flour 488 has the same flourescent colour as calcein AM. There is a high count of Alexa Flour 488 positive events which indicates that the sample contains many cancer cells.

From figure 3.2c, it can be determined that the concentration for that specific experiment would be 556850 cells/mL.

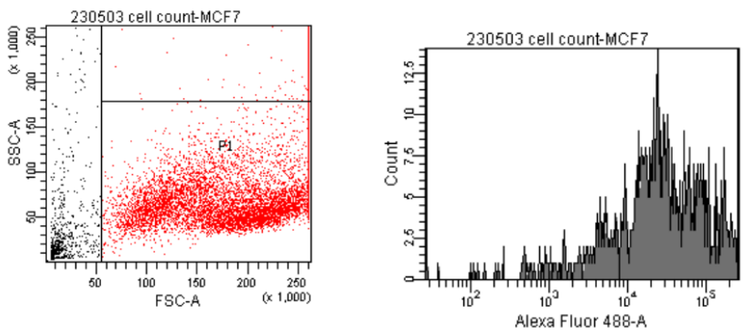

(a) (b)

Tube: MCF7			
Population	#Events	%Parent	%Total
All Events	11,853	####	100.0
P1	11,137	94.0	94.0

(c)

Figure 3.2.: Data taken from FACS with MCF7 cells staind with Calcein AM in PBS buffer. a) Forward scatter plotted on the x-axis and side scatter plotted on the y-axis. Live cells are gated as P1. b) Alexa Flour 488 (representing Calcein AM) plotted on the x-axis and cell count plotted on the y-axis. c) The ratio between the events from figure 3.2a and the gated events

CHAPTER 4

Calculation of mobility ratio with particle separation

The main objectives of this chapter is to get an understanding regarding how to calculate the mobility ratio between cells and polystyrene beads, using MATLAB.

4.1. Background about mobility ratio

The mobility ratio between particles can be measured based on particle separation. With the measurement method used in this thesis, no previous knowledge about viscosity of the fluid, acoustic energy density, flow rate or the length of the channel is needed in order to obtain mobility ratio. By measuring mobility ratios, the difference in mobility between particles can be quantified. Further, it can be used in order to evaluate separation efficiency for different particles. Particles that have similar acoustic mobility will be harder to separate from each other [23]. In this thesis, measuring the mobility ratio will be of importance in order to optimize parameters for particle separation. The ratio will give information about how much faster one particle migrates towards the pressure node when affected by an acoustic standing wave, compared to the other particle.

In this thesis, methods used to measure the mobility ratio have been performed according to a thesis written by Linda Péroux [23]. The equation that is used relates the mobility ratio to the particle path and is derived by Dr. Thierry Baasch, please see equation 4.5 .

Two forces will affect a particle in a channel: the radiation force F_{rad} and the drag force F_{drag}. The Stokes drag force is given by the equation below:

$$\vec{F}_{drag} = -6\pi\eta a v_p(y) \tag{4.1}$$

where η is the dynamic viscosity of the fluid. The drag force affects the particle due to the viscous interactions between the particle and the surrounding medium [1].

The radiation force is given by equation 2.4. If the size of the particle is above a critical size a_c, the radiation force 2.4 will dominate making the particle migrate towards the pressure node [1].

The total force on the particle can be described as:

$$\vec{F}_{tot} = \vec{F}_{rad} + \vec{F}_{drag} = -4\pi\phi k a^3 E_{ac} sin(2ky) - 6\pi\eta a v_p(y) \tag{4.2}$$

At dynamic equilibrium, $F_{tot} = 0$. The velocity of the particle in the y-axis of the channel can therefore be described with the following differential equation:

$$v_p(y) = -\frac{2}{3}\phi\frac{ka^2}{\eta} sin(2ky) E_{ac} \tag{4.3}$$

The mobility ratio of particle 1 over particle 2 can be described as:

$$MR_{1,2} = \frac{\phi_1 a_1^2}{\phi_2 a_2^2} \tag{4.4}$$

where ϕ_1 is the acoustic contrast factor for particle 1 and ϕ_2 is the acoustic contrast factor for particle 2.

The equation that will be used in this thesis, taken from Linda Péroux thesis and derived by Dr. Thierry Baasch relates the mobility ratio to the particle path as follows:

$$MR_{1,2} = \frac{\phi_1 a_1^2}{\phi_2 a_2^2} = \frac{\int_{y_0}^{y_{e1}} (\frac{v_x(y)}{\sin(2ky)}) dy}{\int_{y_0}^{y_{e2}} (\frac{v_x(y)}{\sin(2ky)}) dy} \tag{4.5}$$

with $v_{x(y)}$ being the flow profile of the velocity in the x-direction. The parameters needed to be measured for this equation is the initial position of the pre-focused particle stream y_0 and the two positions of the particle streamlines after main focusing y_{e1} and y_{e2}. Please see figure 4.1 for description of these factors.

4.2. Calculation of mobility ratios using MATLAB

In this thesis, two different types of cells are separated from polystyrene beads in a chip, and multiple pictures are taken as the voltage in the main channel increases to gather as much data as possible. Polystyrene beads of varying sizes are also separated from each other. The pictures like 4.1 are studied in MATLAB, where a number of pixels along the x-axis are averaged, and their intensity is plotted as a function of their y-position, as shown in Figure 4.2. The peaks in the plot represent streamlines, and their width gives an uncertainty as the width of the beam is related to the distribution and variability of the cells. The value of the approximation of the peak position is obtained according to the method shown in figure 4.2a, and these values are presented as d_1 and d_2 in figure 4.2b. The two peaks in 4.2b to the left and right represent the channel walls. The values of d_1 and d_2 are divided by two which gives y_0, y_{e1}, and y_{e2}. With these values, equation 4.5 is used in MATLAB to calculate the mobility ratios.

From figure 4.1, one can see that y_0 is measured in the beginning of the main channel where the pre-focused particles have the same initial position. At the end of the main channel, y_{e1} and y_{e2} can be measured as the particles are separated due to the acoustic standing wave into two different streams.

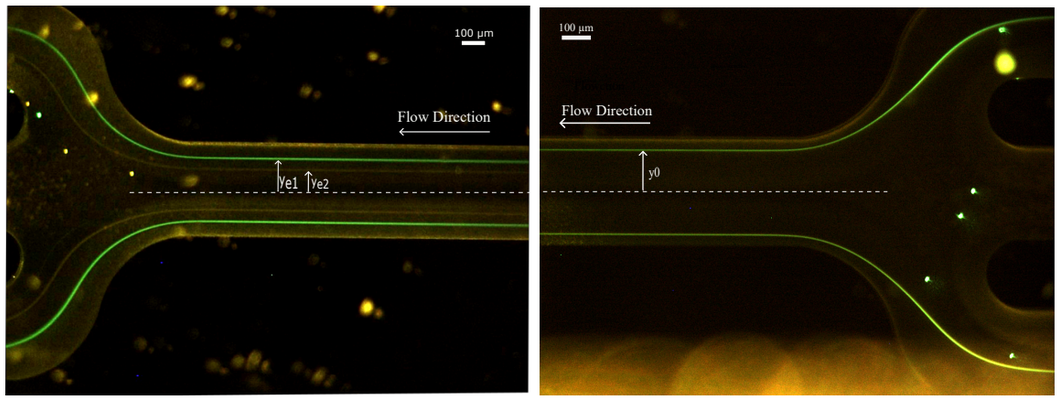

(a) (b)

Figure 4.1.: Red 9.89 μm and green 4.99 μm are separated in 20% Iodixanol. The picture is analysed in MATLAB to obtain the value of y_0, y_{e1} and y_{e2}. The flow in the chip goes from right to left. a) Picture taken at the end of the main channel, the outlet fork. b) Picture taken at the beginning of the main channel, the inlet fork

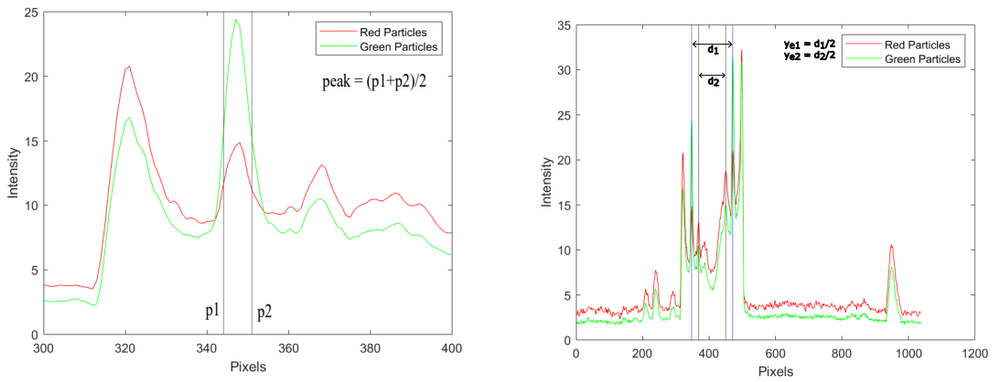

(a) (b)

Figure 4.2.: Red 9.89 μm and green 4.99 μm are separated in 20% Iodixanol, where the peaks represent the streamlines. The averaged pixel intensity is plotted as a function of the y-axis position. a) This intensity curve is zoomed in on the upper green streamline to demonstrate how the width is calculated to obtain the peak position values, seen in b). The width corresponds to 11 pixels = 4 μm. b) The distance between two streamlines for two different particles. The distance is shown as d_1 and d_2, and is divided by two to determine the position of y_{e1} and y_{e2}

The highest separation gap is used in order to determine the mobility ratio. This represents the most extreme condition in which the particles exhibit the most significant separation. If an average mobility ratio would be calculated, it would not represent the devices true separation abilities. The average mobility ratio would weaken the influence of the extreme separation condition.

CHAPTER 5

Methods and results - polystyrene beads

This chapter explains the method used for the set up when separating polystyrene beads in different sizes from each other. Furthermore, the results from three different experiments are provided. In this chapter, we also compare the results in MQ water obtained in this thesis with other results from another master student. The values of the three maximum separation gaps are presented in the tables. However, it is the absolute maximum that is used and compared as this is the most accurate value for the mobility ratio.

5.1. Method used for polystyrene beads

A total flow rate of 200 μL/min (Q_{tot}), inlet splitting ratio of 0.8 (r_{in}) and outlet splitting ratio of 0.2 (r_{out}) are used during these experiments. Camera exposure time is set to 1 second and the temperature of the set-up is controlled by the temperature controller and is never below 24.6°C or above 30°C. Two different buffers are used; MQ water and 20% Iodixanol.

The peak-to-peak voltage in the main channel piezo is set to different values to obtain more data points. Pictures of the inlet and outlet are taken and studied in Matlab. By using MATLAB, y_0, y_{e1} and y_{e2} are measured according to 4.1. The measured values are obtained from the intensity curve, see 4.2. Further, equation 4.5 is used in MATLAB in order to obtain the mobility ratios.

The particles are diluted to a concentration of 0.0025%w/v, from the original concentration of 2.5%w/v from manufacturer. This corresponds to a volume of 0.0025 mL for each particle in a solution of 4.995 mL MQ water.

5.2. Red 9.89 μm and green 5.19 μm in MQ water and 20% Iodixanol

In this experiment, red 9.89 μm and green 5.19 μm particles were separated in two different buffers. The mobility ratios for both MQ water and 20% Iodixanol can be seen in table 5.1. The voltage in the main channel piezo is altered between 3V to 10V, with steps of 0.5V in MQ water and in 20% Iodixanol.

Figure 5.1 is shown as a subplot and shows the mobility ratio in MQ water and 20% Iodixanol.

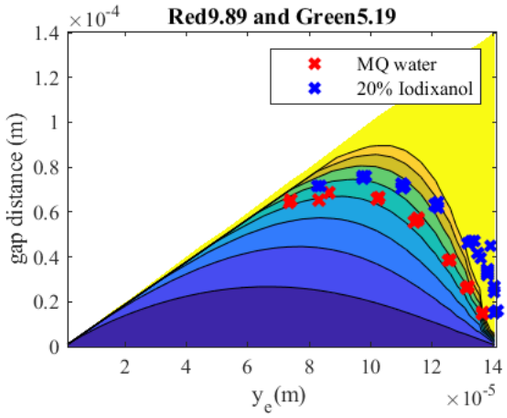

Figure 5.1.: The mobility ratio for red 9.89 μm and green 5.19 μm polystyrene particles in MQ water presented as red crosses, and in 20% Iodixanol presented as blue crosses. The values for the isolines are 1,1.5,2,2.5,3,3.5,4,4.5,5

Table 5.1.: Mobility ratios for the three highest separation gaps for red 9.89 μm and green 5.19 μm in two different solutions. The highest gap value is presented in bold

Particles [μm]	**Mobility ratio - MQ**	**Mobility ratio - 20% Iodixanol**
9.89/5.19	3.02	3.67
	3.10	3.78
	3.26	**3.80**

5.3. Red 9.89 μm and green 7.81 μm in MQ water and 20% Iodixanol

In this experiment, red 9.89 μm and green 7.81 μm particles were separated in two different buffers. The values of the mobility ratios can be seen in table 5.2. The voltage in the main channel piezo is altered between 4V to 9.5V, with steps of 0.5V in MQ water. In 20% Iodixanol, the voltage is altered between 8V to 19V with steps of 1V.

For these experiments, a fiber was found inside the chip when the experiment started, see figure A.3 and A.4 in Appendix.

Figure 5.2 is shown as a subplot and shows the mobility ratio in MQ water and 20% Iodixanol.

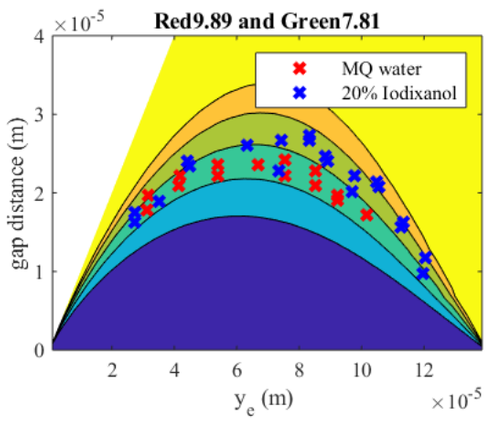

Figure 5.2.: The mobility ratio for red 9.89 μm and green 7.81 μm polystyrene particles in MQ water presented as red crosses, and in 20% Iodixanol presented as blue crosses. The values for the isolines are 1,1.3,1.4,1.5,1.6,1.7

Table 5.2.: Mobility ratios for the three highest separation gaps for red 9.89 μm and green 7.81 μm in two different solutions. The highest gap value is presented in bold

Particles [μm]	**Mobility ratio - MQ**	**Mobility ratio - 20% Iodixanol**
9.89/7.81	1.48	1.52
	1.49	1.58
	1.50	**1.59**

5.4. Red 4.99 μm and green 7.81 μm in MQ water and 20% Iodixanol

In this experiment, red 4.99 μm and green 7.81 μm particles were separated in two different buffers. The mobility ratios can be seen in table 5.3. The voltage in the main channel piezo is altered between 3V to 7.5V, with steps of 0.5V in MQ water. In 20% Iodixanol, the voltage is altered between 5.5V to 14V with steps of 0.5V.

Figure 5.3 is shown as a subplot and shows the mobility ratio in MQ water and 20% Iodixanol.

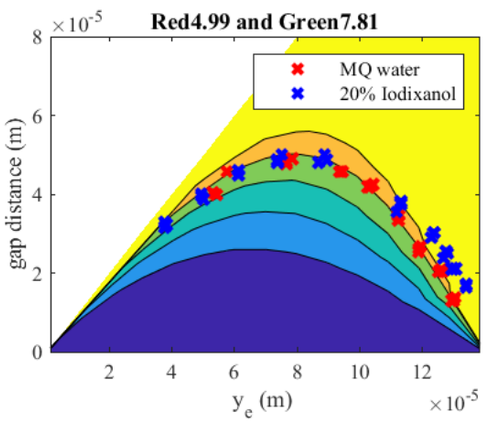

Figure 5.3.: Showing the mobility ratio for red 4.99 μm and green 7.81 μm polystyrene particles in MQ water represented as red crosses, and in 20% Iodixanol represented as blue crosses. The values for the isolines are 1, 1.5, 1.75, 2, 2.25, 2.5

Table 5.3.: Mobility ratios for the three highest separation gaps for red 4.99 μm and green 7.81 μm in two different solutions. The highest gap value is presented in bold

Particles [μm]	**Mobility ratio - MQ**	**Mobility ratio - 20% Iodixanol**
4.99/7.81	2.22	2.17
	2.24	2.20
	2.27	**2.25**

5.5. Comparison of mobility ratio

In table 5.4, the mobility ratios obtained where the gap is the highest are presented, for three different experiments in two different buffers.

The results obtained in this thesis are compared to the results from another master student, Linda Péroux, here referred to as "Reference" [23]. In the table below, 5.5, the acoustic mobility ratio for the highest gap are compared to reference values to draw a conclusion about the accuracy. Both experiments are made in MQ water.

Further, figure 5.4 representing a bar graph can be seen with the values obtained of the acoustic mobility ratio for all of the experiments in this thesis, compared to reference (values by another master student, Linda Péroux [23]).

Table 5.4.: The results obtained in this thesis are presented in the table below. The mobility ratio in MQ water vs 20% Iodixanol for three different experiments

Particles [μm]	Mobility ratio - MQ	Mobility ratio - 20%
Red9.89/Green5.19	3.26	3.80
Red9.89/Green7.81	1.50	1.59
Red4.99/Green7.81	2.27	2.25

]

Table 5.5.: Mobility Ratios for different particles in MQ water. Reference of the mobility ratio obtained at the highest gap are taken from another master student which are also presented

Particles [μm]	Mobility ratio - MQ	Reference - MQ
Red9.89/Green5.19	3.26	3.26
Red9.89/Green7.81	1.50	1.50
Red4.99/Green7.81	2.27	2.22

]

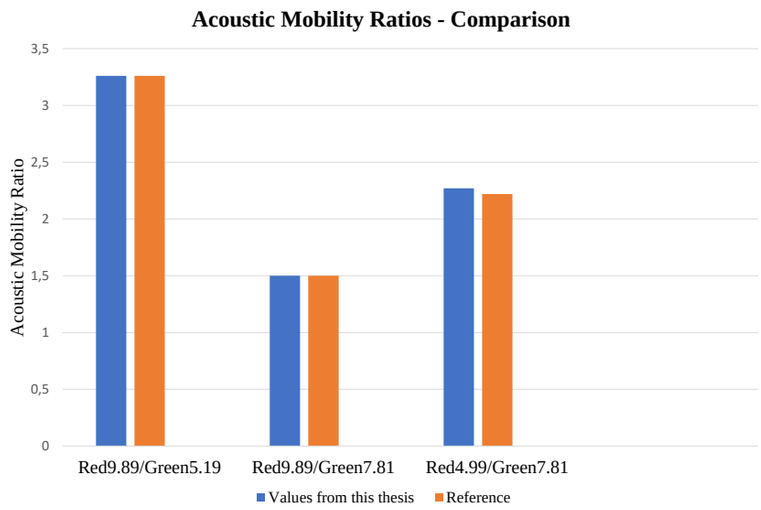

Figure 5.4.: The mobility ratio in this thesis is compared with the values obtained by another master student, [23]. The particles that are compared are red 9.89 μm with green 5.18 μm, red 4.99 μm with green 7.81 μm and red 4.99 μm with green 7.81 μm polystyrene particles, in MQ water

5.6. Reference experiment with fiber in the chip

During the experiment involving red 9.89 μm and green 7.18 μm beads, a fiber was observed at the outlet fork in the acoustophoretic chip despite the attempts of rinsing the chip. To evaluate the impact of the fiber on the results, a reference experiment is made using red 9.89 μm and green 5.19 μm beads with the fiber still present in the chip. This reference experiment is aimed to compare the outcomes with a previous experiment that utilized the same bead sizes (red 9.89 μm with green 5.19 μm) but was performed without the fiber in the chip. The goal is to determine whether the fiber has any influence on the results obtained.

Pictures taken with the fiber inside the end of the outlet fork is compared with the picture taken without the fiber inside the chip, see figure 5.5. The mobility ratios in MQ water for both experiments are shown as a subplot in figure 5.6. In table 5.6, the maximum values of the mobility ratios are shown.

The reference experiment is conducted in MQ water. The voltage in the main channel piezo is altered between 3.5V to 9V, with steps of 0.5V

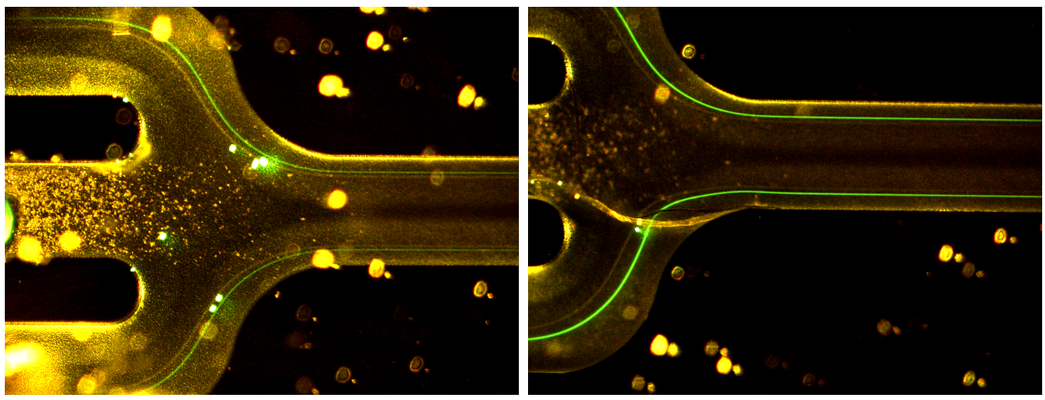

(a) (b)

Figure 5.5.: Red 9.89 μm with green 5.19 μm in MQ water. The voltage in the main channel piezo is 3V. a) Picture without a fiber in the end of the outlet fork of the chip. b) The reference experiment with fiber in the end of the outlet fork of the chip

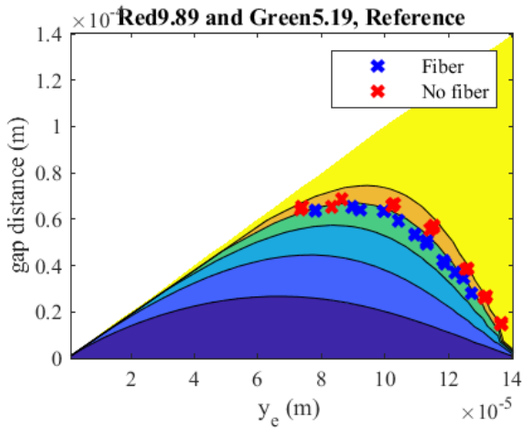

Figure 5.6.: Subplot with red 9.89 μm with green 5.19 μm beads in MQ water. The blue crosses represents the values with the fiber. The red crosses represents the values without the fiber. The values for the isolines are 1,1.5, 2,2.5,3, 3.5

Table 5.6.: Mobility ratio for the highest separation gap for particles 9.89 μm and 5.19 μm without a fiber in the chip are compared to the mobility ratio obtained for the same particles, with a fiber in the chip. Both experiments are made in a buffer of MQ water

Particles [μm]	**Mobility ratio - No fiber**	**Mobility Ratio - Fiber**
9.89/5.19	3.26	3.13

5.7. Discussion

The results made in MQ water are compared to the results accomplished by another master student, Linda Péroux, in her thesis "Pushing the boundaries of acoustic particle separation: achieving high-throughput, avoiding spillover effects, investigating the effects of the particle concentration, and measuring acoustic properties" [23].

The concentration of particles used in this experiment (0.0025% w/v) is relatively low, which may explain why the bands were not very visible. In comparing the red particles (9.89) to the green particles (5.19) as an example, the green appear more intense. The reason could be because the manufacturer-provided concentration is expressed as % weight per volume,

making the amount of red particles lower than the green particles since the former are larger. In Appendix A, it is clearly seen in the figures that the red are less visible.

In a related experiment [23], they tested different particle concentrations to determine if concentration affected separation. The results showed that a maximum particle concentration of 0.005% w/v and a minimum concentration of 0.0005% w/v did not affect separation. However, at higher concentrations, apparent acoustic energy density increased, hindering particle separation, as evidenced by the separation curve. At higher concentrations, particles are closer together and more likely to interact with each other.

In comparing the average mobility ratio obtained in this thesis to that obtained by Linda Péroux [23], our results are in agreement with Linda Péroux. The variation was below 2.23% for all experiments. The small difference in mobility ratio for red 9.89 μm with green 7.81 μm might appear because of the acoustic properties of the particles, such as shape and size, can be slightly different for different experiments depending on their structure and composition. There can also be small differences in the particle concentrations used - as another concentration than the one from the manufacturer was used, there could have appeared errors in particle concentration measurements. The values from Péroux were compared with reference values obtained from particle tracking, another method for measuring mobility ratio. Overall, the results obtained in this thesis are reasonable.

During the experiment involving red 9.89 μm and green 7.81 μm particles, a fiber was discovered in the chip at the start of the experiment. We tried to clean the chip by rinsing it several times as well as taking off the chip from its place to rinse it. Despite our attempts to clean the chip, the fiber remained in place. However, it was determined that the presence of the fiber did not impact the obtained results, as they were consistent with the findings of Linda Péroux. Additionally, since the fiber was located at the end of the main channel, it did not affect the particle separation process. Moreover, a reference experiment was conducted using red 9.89 μm and green 5.19 μm particles with the fiber present in the chip, in order to compare the results with those obtained without the fiber. Remarkably, the mobility ratio remained unchanged, both with and without the fiber.

Equation 4.5 is independent of voltage, indicating that changing the voltage does not affect the results. Therefore, voltage can be adjusted to obtain more data points.

Analyzing table 5.4, it can be concluded that there is no significant difference in mobility ratio between red 4.99 μm with green 7.81 μm particles in MQ water vs 20% Iodixanol. However, there is a difference between red 9.89 μm with green 7.81 μm as well as red 9.89 μm and green 5.19 μm particles. In both cases, the mobility ratio is higher in 20% Iodixanol, indicating that the particles move more quickly relative to each other in this medium than in MQ water when subjected to acoustic forces. This suggests that particles are more easily separated in 20% Iodixanol which in turn indicates that they have different material properties.

CHAPTER 6

Methods and results - cell lines

In this chapter, the method used for separating DU145 cells from polystyrene beads, and MCF7 cells from polystyrene beads, are presented. Additionally, the results obtained regarding the mobility ratios between these cell lines and polystyrene beads in different buffers are presented.

6.1. DU145 cell line for buffer optimization

6.1.1. Method used for DU145 cell line

DU145 cells are cultured according to standard procedure. 50 μL cells at a concentration around roughly 556850 cells/mL according to FACS, are stained with 7 μL calcein AM and 10 μL polystyrene beads are added to the sample, in a solution of 1mL of the buffer used. The voltage in the main channel piezo is swept between different voltages. The frequency is constant at 4.86MHz in the prefocusing channel and 1.990 MHz in the main channel. The total flow rate is held constant at 50 μL/min (Q_{tot}) and r_{in} at 0.8 and r_{out} at 0.2. The amplitude in the prefocusing channel is held constant at 2.5V. Camera exposure time is set to 1 second and the temperature of the set-up is controlled by the temperature controller. The temperature is never below 24°C or above 30°C.

The concentration of the polystyrene particles from the manufacturer are 2.5 %w/v. The concentration used in this experiment after dilution is 0.00236 %w/v.

For these experiments, three polystyrene beads with different sizes are used; 9.89 μm, 7.81 μm and 4.99 μm. Three different buffers are used; PBS, 10% Iodixanol and 20% Iodixanol.

6.1.2. 9.89 μm polystyrene beads with DU145 cells

In figure 6.1, a subplot for red polystyrene beads with the size of 9.89 μm with DU145 beads are plotted. Three different experiments were performed, with three different buffers: PBS, 10% Iodixanol, and 20% Iodixanol. In table 6.1, the mobility ratios for the three biggest gap distances in different buffers are represented.

To calculate the mobility ratio, the mobility of the cells are divided with mobility of the polystyrene beads.

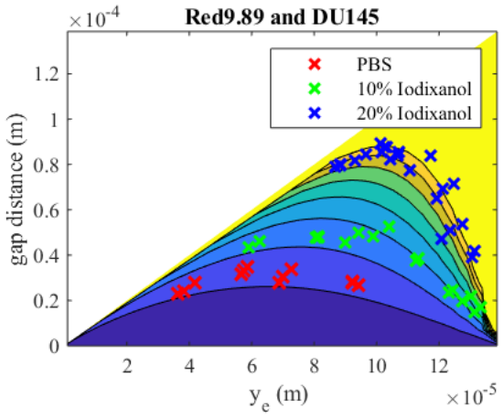

Figure 6.1.: Subplot for three different expeirments made with DU145 cells and 9.89 μm in PBS shown as red crosses, 10% Iodixanol shown as green crosses, and 20% Iodixanol shown as blue crosses. The isolines represent mobility ratio 1,1.5,2,2.5,3, 3.5,4, 4.5, 5, 5.5 from bottom and up.

Table 6.1.: Mobility ratios for the three highest separation gaps for DU145 cells and red 9.89 μm beads in three different solutions. The highest gap value is presented in bold

Buffer	**MR (DU145, Red9.89)**
PBS	1.76
	1.78
	1.80
10%	2.39
	2.40
	2.69
20%	4.67
	4.88
	5.10

6.1.3. 7.81 μm polystyrene beads with DU145 cells

In this experiment, DU145 cells are used with 7.81 μm polystyrene beads. In figure 6.2, a subplot showing the separation curves for PBS and 10% Iodixanol is presented. In table 6.2, the mobility ratios for the biggest gap distance for two different buffers are presented. Only a few values were obtained in PBS as the cells ran out during the experiment.

To calculate the mobility ratios, the mobility of the cells are divided with mobility of the polystyrene beads.

For the experiment in 10% Iodixanol, a fiber was found inside the chip when the experiment started.

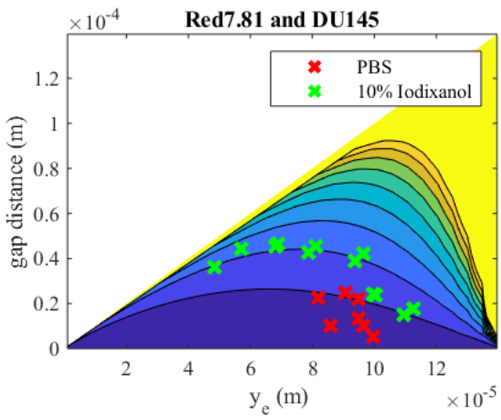

Figure 6.2.: The separation curve obtained for the red 7.81 μm and DU145 cells in PBS, shown as red crosses, and in 10% Iodixanol shown as green crosses. The graph shows the mobility ratios for voltages swept between 9V to 14V with steps of 1V with one picture taken for every voltage in PBS. In 10% Iodixanol, the voltages are swept between 4V and 9V with steps of 1V, and two pictures taken for every voltage. The isolines represent the mobility ratio 1,1.5,2,2.5,3, 3.5,4, 4.5, 5, 5.5 from the bottom line and up.

Table 6.2.: Mobility ratios for the three highest separation gaps for DU145 cells and red 7.81 μm beads in two different solutions. The highest gap value is presented in bold

Buffer	**MR (DU145, Red7.81)**
PBS	1.48
	1.51
	1.67
10%	2.24
	2.32
	2.42

6.1.4. 4.99 μm polystyrene beads with DU145 cells

In this experiment, DU145 cells are used with 4.99 μm polystyrene beads. In figure 6.3, a plot showing the separation curve in PBS presented. In table 6.3, the mobility ratio for the three highest gap distances are presented.

To calculate the mobility ratio, the mobility of the polystyrene beads are divided with mobility of the cells.

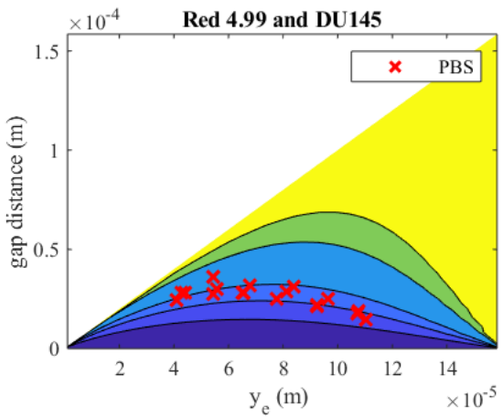

Figure 6.3.: The separation curve obtained for the red 4.99 μm with DU145 cells in PBS, shown as red crosses. The graph shows the mobility ratios for voltages swept between 3V to 5.5V with steps of 0.5V with three picture taken for every voltage in PBS. The isolines represent the mobility ratio 1,1.5,1.6,1.7,2, 2.5 from the bottom line and up

Table 6.3.: Mobility ratios for the three highest separation gaps for DU145 cells and red 4.99 μm beads in one solutions. The highest gap value is presented in bold

Buffer	**MR (Red4.99, DU145)**
PBS	1.61
	1.67
	1.89

An experiment for DU145 cells with red 4.99 μm polystyrene beads in a buffer of 20% Iodixanol was also performed. However, there was no separation and the gap was always around 0. In figure 6.4a, it can be seen that the red particles follow the green cells, and no separation occurs which implies a mobility ratio around 1. In the linegraph plot 6.4b, the different peaks representing the red particle beam and the cell beam cannot be distinguish either. This also implies that the particles follow the cells.

Two different figures are presented here, taken at two different voltages, to strengthen the thesis that the cells are where the particles are and that it is hard two see the different beams. The amplitude in the main channel is 4.5V for figure 6.4 and 6.5V for figure 6.5

For this experiment, still 3 figures were taken for every voltage, where the amplitude in the main channel altered between 1.6V and 5V with steps of 0.5-1.5V.

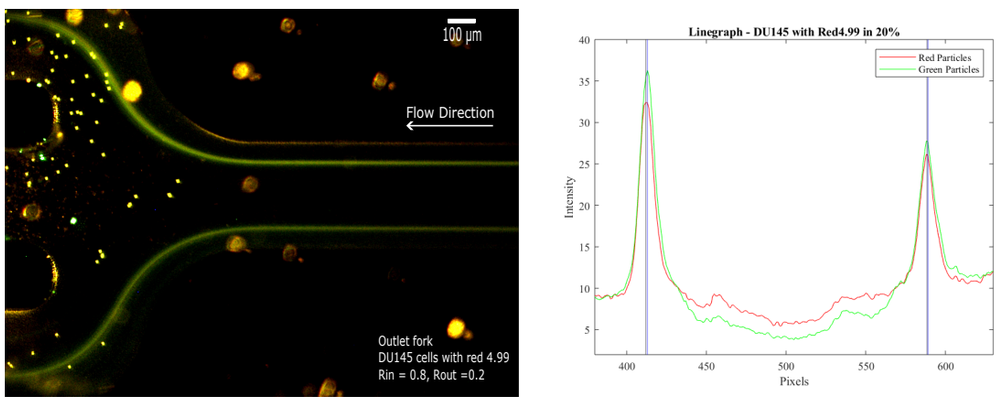

(a) (b)

Figure 6.4.: Experiment for DU145 cells stained with green Calcein, and red 4.99μm particles in a buffer of 20% Iodixanol. The amplitude in the main channel is 4.5V. a) Picture taken at the outlet fork in the main channel. The particles cannot be distinguished from the cells. The flow goes from right to left in the channel. b) Linegraph plotted in Matlab, corresponding to figure 6.4a. The four different lines that represent y_{e1} and y_{e2} cannot be distinguished

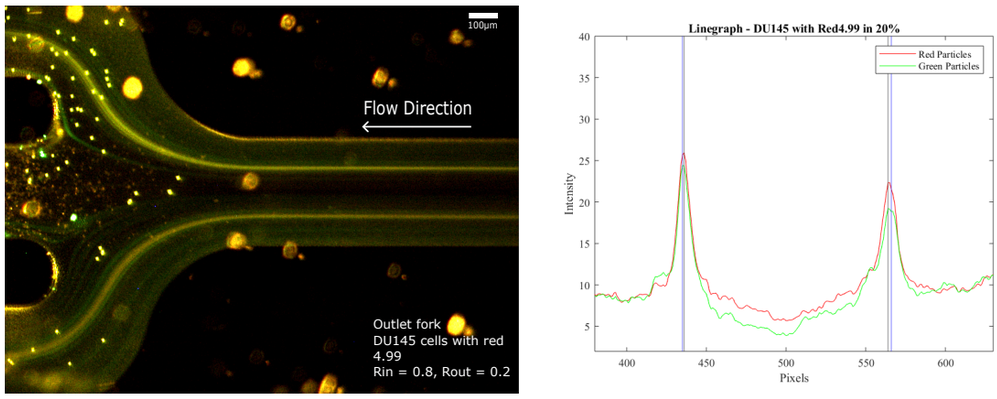

(a) (b)

Figure 6.5.: Experiment for DU145 cells stained with green Calcein AM, and red 4.99 μm particles in a buffer of 20% Iodixanol. The amplitude in the main channel is 6.5V. a) Picture taken at the outlet fork in the main channel. The particles cannot be distinguished from the cells. The flow goes from right to left in the channel. b) Linegraph plotted in Matlab, corresponding to figure 6.5a. The four different lines that represent y_{e1} and y_{e2} cannot be distinguished

6.1.5. Test of flow rate

As a lower total flow rate, Q_{tot}, is used with these experiments compared to when only doing experiments with polystyrene beads, a test is performed to control if the flow rate would affect the beads. The test is performed on red 9.89 μm with green 5.19 μm in MQ water. Q_{tot}=50 μL/min is used for experiments with cells and Q_{tot}=200 μL/min is used for beads.

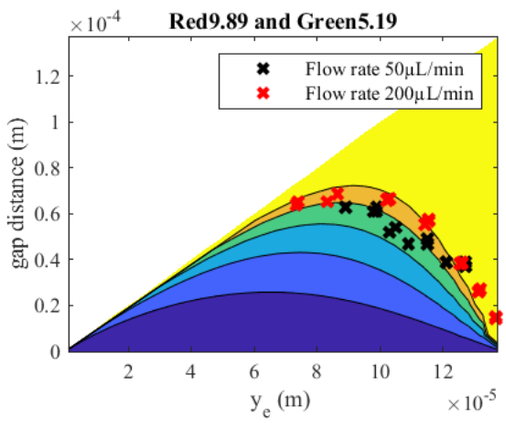

Figure 6.6.: Subplot for two different experiments made with red 9.89 μm and green 5.19 μm in MQ water for 2 different flow rates. With a flow rate Q_{tot}=200 μL/min presented as red crosses and a flow rate Q_{tot}=50 μL/min presented as black crosses The isolines represent the mobility ratio 1,1.5,2,2.5, 3, 3.5 from bottom and up

Table 6.4.: Mobility ratio for the highest separation gap for particles red 9.89 μm with green 5.19 μm in MQ water at two different flow rates - Q_{tot}=50 μL/min and Q_{tot}=200 μL/min - are compared.

Particles [μm]	**Q_{tot}=50 μL/min**	**Q_{tot}=200 μL/min**
9.89/5.19	3.11	3.26

6.1.6. Discussion for DU145 cells

In the experiment involving DU145 cells and 9.89 μm particles in 10% buffer, only two pictures for each voltage instead of three were taken due to an issue with the set-up. The initial challenge was the presence of fibers inside the chip, which were successfully removed after cleaning. However, another issue came up when we realized that the setup could not transition directly from a higher total flow rate, automatically set at 500 μL/min when starting the set up, to the flow rate required for cell experiments (50 μL/min). This abrupt change did that the system did not stabilize properly. To deal with this problem, we gradually reduced the total flow rate in increments of 50 μL/min until we reached the desired flow rate. However, these problems resulted in a depletion of cells during the experiment, hence less amount of cells and time to run with. Despite this, the impact on the results is expected to be minimal as multiple pictures are taken only to reduce uncertainties.

When comparing the mobility ratio of DU145 cells with 9.89 μm polystyrene particles in different buffers, a difference in mobility ratio can be observed. The mobility ratios obtained in PBS, 10% Iodixanol, and 20% Iodixanol buffers were 1.80, 2.69, and 5.10, respectively. Therefore, it can be concluded that the highest mobility ratio is achieved when 20% Iodixanol is used as a buffer, resulting in better separation.

When it comes to DU145 cells with 7.81 μm polystyrene beads, the mobility ratio is higher when adding Iodixanol (10% Iodixanol) compared to PBS. Hence same result as the experiment using 9.89 μm particles. Overall, this variation in mobility ratio could be due to the different acoustic properties of the buffers, which can affect the mobility of particles and cells differently, with PBS being less viscous than Iodixanol. We did not get as many data points in PBS as in 10% Iodixanol for the expeirment with 7.81 μm beads, as we ran out of cells during the experiments due to fibers in the chip.

The results given from the experiment for DU145 cells and red 4.99 μm polystyrene beads are only obtained from a PBS-buffer. The reason to this is because the cells and the particles followed each other and could not be separated in a buffer of 10% Iodixanol. No gap between them could be seen, which is clearly showed in figure 6.4 and 6.5. From this it can be concluded that the mobility ratio is 1 in 10% Iodixanol.

Only two out of the three different buffers were tested for the experiments involving 7.81 μm and 4.99 μm particles. This was due to various challenges encountered during the experiments, such as the presence of fibers in the chip and difficulties in stabilizing the system, as previously described. Unfortunately, these issues led to the depletion of cells during the experiments, preventing us from getting any data for all three buffers.

For the experiment with DU145 cells with 7.81 μm polystyrene beads in 10% Iodixanol, a fiber was found at the end of the outlet fork in the chip when I already had started the experiment. Despite our attempts to clean the chip, the fiber did not go away. However, since this most likely was the same fiber as the run with red 9.89 μm with green 7.81 μm beads (since the experiments were done after each other), this fiber did not affect the result. This can be proved by the reference run with red 9.89 μm with green 5.19 μm beads that I did dto evaluate how or if the fiber affected the result - which it did not do.

A test was conducted to examine the impact of flow rate on the behavior of the beads. A flow rate of Q_{tot}=200 μL/min was compared to a flow rate of Q_{tot}=50 μL/min. The latter

one corresponds to the flow rate employed during the experiments with cell lines. A lower total flow rate was used as the cells need to be handled more delicately than the rigid and stable polystyrene beads. As illustrated in figure 6.6, the two lines are closely align with each other, indicating that the mobility ratio remains nearly unchanged when the flow rate is reduced. This observation suggests that the lower flow rate has negligible effects on the beads and is therefore a suitable choice.

6.2. MCF7 cell line for buffer optimization

6.2.1. Method used for MCF7 cell line

MCF7 cells are cultured according to standar procedure. 50 μL cells at a concentration around roughly 556850 cells/mL according FACS, are stained with 7 μL Calcein AM and 10 μL polystyrene beads are added to the sample, in a solution of 1mL of the buffer used. The voltage in the main channel piezo is swept between different voltages. The frequency is constant at 4.86MHz in the prefocusing channel and 1.990 MHz in the main channel. The total flow rate, Q_{tot} is held constant at 50 μL/min and r_{in} at 0.8 and r_{out} at 0.2. The amplitude in the prefocusing channel is held constant at 2.5V. Camera exposure time is set to 1 second and the temperature of the set-up is controlled by the temperature controller. The temperature is never below 24°C or above 29°C.

The concentration of the polystyrene particles from the manufacturer are 2.5 %w/v. The concentration used in this experiment after dilution is 0.00236 %w/v. Three different buffers are used - PBS, 10% Iodixanol and 20% Iodixanol.

6.2.2. 9.89 μm polystyrene beads with MCF7 cells

Experiments for MCF7 cells with red 9.89 μm polystyrene beads in three different buffers - PBS, 10% Iodixanol and 20% Iodixanol, were performed.

No separation is seen in PBS and the gap is always around 0. In figure 6.7a it can be seen that the red particles follow the green cells, and no separation occurs. In the plot in figure 6.7b the different peaks representing the red particle beam and the cell beam cannot be distinguish either. This also shows that the particles follow the cells, which implies a mobility ratio of 1.

Two different figures are presented here, taken at two different voltages, to strengthen the hypothesis that the cells are where the particles are and that it is hard two see the different beams. The amplitude in the main channel is 2V for figure 6.7 and 3.5V for figure 6.8

For this experiment, still 3 figures were taken for every voltage, where the amplitude in the main channel alters between 1V and 6V with steps of 0.5-1V.

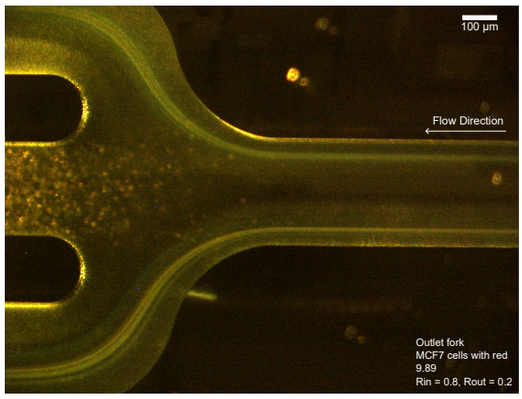

(a)

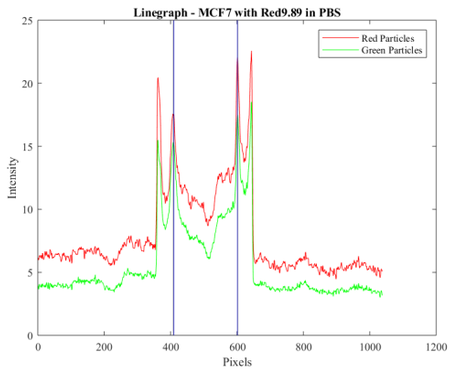

(b)

Figure 6.7.: Experiment for MCF7 cells stained with green Calcein AM, and red 9.89 μm particles in a buffer of PBS. The amplitude in the main channel is 2V. a) Picture taken at the outlet fork in the main channel. The particles cannot be distinguished from the cells. The flow goes from right to left in the channel. b) Linegraph plotted in Matlab, corresponding to figure 6.7a. The four different lines that represent y_{e1} and y_{e2} cannot be distinguished

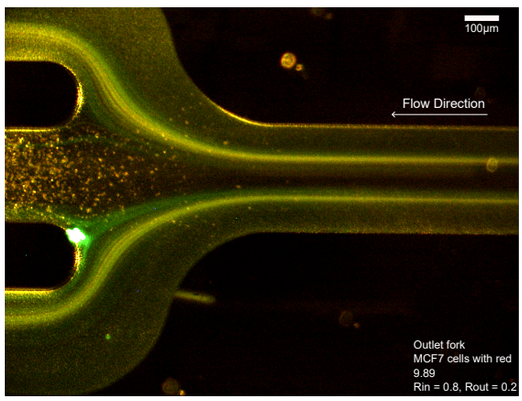

(a)

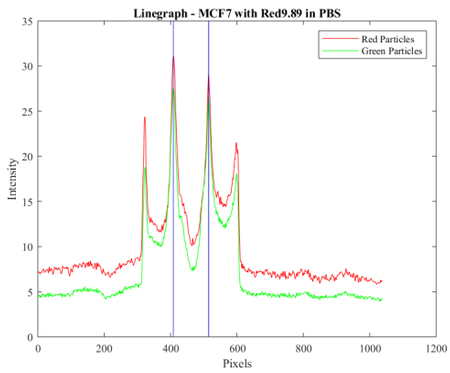

(b)

Figure 6.8.: Experiment for MCF7 cells stained with green Calcein, and red 9.89 μm particles in a buffer of PBS. The amplitude in the main channel is 3.5V. a) Picture taken at the outlet fork in the main channel. The particles cannot be distinguished from the cells. The flow goes from right to left in the channel. b) Linegraph plotted in Matlab, corresponding to figure 6.8a. The four different lines that represent y_{e1} and y_{e2} cannot be distinguished

For the experiments made in the buffers 10% and 20% Iodixanol, the MCF7 cells never moved to the center outlet. In both figure 6.9 and figure 6.10, the red polystyrene beads move to the center while the cells move even closer to the side, meaning that they have a negative contrast factor.

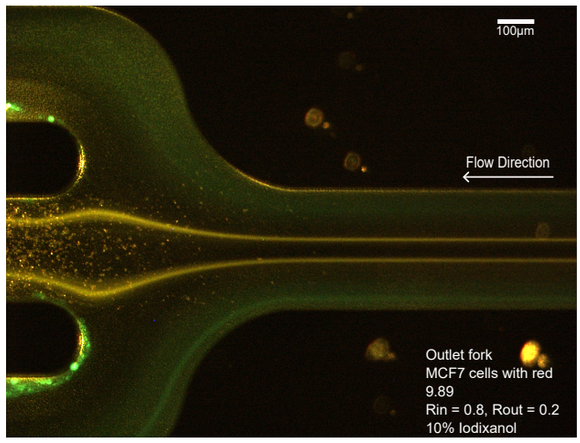

Figure 6.9.: Picture taken at the outlet fork in the main channel at an amplitude of 3.5V in the main channel, for MCF7 cells stained with Calcein AM and red 9.89 μm polystyrene beads in 10% Iodixanol as a buffer. The red particles are clearly separated from the green cells.

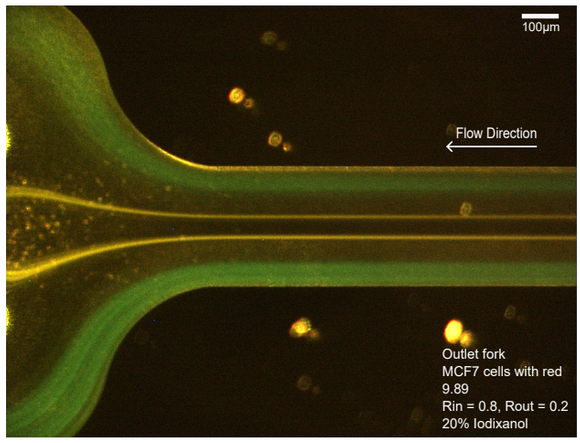

Figure 6.10.: Picture taken at the outlet fork in the main channel at an amplitude of 5V in the main channel, for MCF7 cells stained with Calcein AM and red 9.89 μm polystyrene beads in 20% Iodixanol as a buffer. The red particles are clearly separated from the green cells.

6.2.3. Discussion for MCF7 cells

MCF7 cells with 9.89 μm polystyrene beads in PBS could not be separated. The cells followed the particles and the different streams could not be distinguished, which is clearly showed in figure 6.7 and in figure 6.8. This implies a mobility ratio of 1.

Figure 6.9 and figure 6.10 illustrate a noteworthy phenomenon observed in the presence of a buffer containing 10% and 20% Iodixanol, respectively. The observed behavior of the MCF7 cells deviates from their expected movement towards the center, and moved even closer to the sides. This behaviour that is seen shows that the acoustic contrast factor changed for MCF7 cells when adding Iodixanol. The cells obtained a negative acoustic contrast factor, thereby preventing their migration towards the center and resulted in better separation.

The mobility ratios cannot be measured for the MCF7 cells since the curves that are plotted in MATLAB do not apply for negative contrast factors. The cells are very close to the walls which leads to hydrodynamic interactions. The walls also create additional forces on the cells which in turn can influence the motion of the cells. As a result, the mobility ratios of the cells may be altered which will make it hard to analyze.

CHAPTER 7

Conclusions

7.1. Concluding remarks

The main objective of this thesis was to compare the mobility ratios in MQ water for differently sized polystyrene beads with results obtained from another master student, as well as separate them using different buffers. Furthermore, to evaluate the mobility ratio for DU145 cells and MCF7 cells in different buffers. By cultivating and growing these cancer cells, they could be used together with polystyrene beads in an acoustofludic chip in order to evaluate the mobility ratio. This was done by measuring the displacement of the particles and cells from their initial positions.

Comparisons between polystyrene beads were drawn between the mobility ratios observed in MQ water and those obtained by another master student, Linda Péroux, also in MQ water, yielding similar outcomes. Moreover, from this thesis we can conclude that the mobility ratios generally exhibited higher values in a buffer of 20% Iodixanol. This discovery implies that the material properties of large and small particles, despite sharing the material composition of polystyrene beads, are influenced by the surrounding buffer medium. This leads to the conclusion that they differ in material properties. This unexpected outcome should be further investigated, as polystyrene beads often are used as reference material in research.

When examining DU145 cells, separation was observed with 9.89 μm beads for all buffer conditions, with particularly favorable results in 20% Iodixanol. For 7.81 μm beads, the most effective separation was achieved in 10% Iodixanol compared to PBS. In contrast, 4.99μm beads had optimal separation in PBS rather than 20% Iodixanol. The reason for the differences in separation efficiency between 9.89 μm, 7.81 μm and 4.99 μm beads in PBS is associated to their respective velocities relative to the cells. 4.99 μm move slower than cells in PBS, compared to the bigger particles that move faster than cells. However, when introducing Iodixanol to the buffer, the cells velocity decreases. This means that the cells will follow the slow 4.99 μm beads more, while there will be a better separation for the bigger beads. When it comes to MCF7 cells, the best separation was seen in 10% Iodixanol and even a little bit better in 20% Iodixanol. For these experiments, we can conclude that we got a sign change for the acoustic contrast factor when adding Iodixanol, giving optimal separation.

Since we were able change the acoustic contrast factor for MCF7 in 10% and 20% Iodixanol, it would be possible to separate these cells from DU145 cells in these two buffers.

Working with cells proved to be more challenging and time-consuming than initially anticipated. Firstly, due to their biological nature, cells need to be handled delicately and are very fragile. Moreover, tasks that were initially observed as relatively straightforward, such as identifying suitable cell staining methods or determining optimal bead concentrations, consumed more time than expected. Lastly, the evaluation of images to measure mobility ratios proved to be more demanding than first anticipated. Mostly because the stream of the cells were very wide, as can be seen on all the pictures, and therefore hard do evaluate. Additionally, several issues came up during the experimental setup, such as the presence of fibers in the chip. This unexpected occurrence resulted in a depletion of the cells that were intended to be used for the experiment on that particular day. Since cells require cultivation and growth, we had to endure a delay of several days before being able to repeat the same experiment. With this said, I for sure have the experience of knowing that research take much longer time than expected, especially when working with cells, and that it takes a lot of planning to do only one experiment.

On the whole, this thesis presented different ways to optimize buffers for separation of DU145 cells from differently sized polystyrene beads, as well as for MCF7 cells. This gives information and knowledge about how these cells behave and can be used in further research for separating these cells from other cell lines. Additionally, measuring mobility ratios provides valuable result into the separation of cells or particles within a particular buffer medium and can be used for further investigations of separation efficiency.

7.2. Future research

Following experiments and improvements for separation of cells and particles might be of interest to investigate in the future.

- Further experimentation should be made to test other buffers for the separation of DU145 cells with beads of varying sizes. The objective is to identify a buffer that can achieve even better separation than the ones investigated in this thesis.

- An interesting experiment would be to explore the separation of MCF7 cell lines from other breast cancer cell lines considering their similar acoustophoretic mobilities in water.

- More cells could be investigated. In this thesis, our hope was to test alpha- and beta cell lines as well. The goal is to separate these cell lines not only from polystyrene beads but also from each other.

- In the future, an improvement would be to test the concentration of cells at least one or two more times to get a better understanding of the concentration levels.

Bibliography

[1] Bruus H. "Acoustofluidics 10: Scaling laws in acoustophoresis". In: *Lab on a Chip.* 12.9 (2012). DOI: https://doi.org/10.1039/C2LC21261G.

[2] Lenshof A. "Acoustic standing wave manipulation of particles and cells in microfluidic chips". In: (2009). PhD Thesis.

[3] Urbansky A, Ohlsson P, Lenshof A, Garfoalo F, Scheding S and Laruell T. "Rapid and effective enrichment of mononuclear cells from blood using acoustophoresis". In: *Scientific Repports.* 7.3 (2017). DOI: https://doi.org/10.1038/s41598-017-17200-9.

[4] Laurell T and Nilsson A. "Continuous separation of cells and particles in microfluidic systems". In: *Chemical Society Reviews.* 39.3 (2010), pp. 1203–1217.

[5] Laurell T, Petersson F and Nilsson A. "Chip integrated strategies for acoustic separation and manipulation of cells and particles". In: *Chemical Society Reviews.* 36.3 (2007), pp. 496–506.

[6] Undvall E. "Isolation of Circulating Tumor Cells with Acoustophoresis: Towards a biomarker assay for prostate cancer". In: (2022).

[7] Magnusson C, Augustsson A, Lenshof A, Ceder Y, Laurell T and Lilja H. "Clinical-scalecell-surface-marker independent acoustic microfluidic enrichment of tumor cells from blood". In: *Analytical chemistry.* 89.22 (2017), 11954–11961. DOI: https://doi.org/10.1038/s41598-017-17200-9.

[8] Fan Y, Wang X, Ren J, Lin F and Wu J. "Recent advances in acoustofluidic separation technology in biology". In: *Microsyst Nanoeng.* 8.94 (2022). DOI: 10.1038/s41378-022-00435-6.

[9] Wang G, Yang F and Zhao W. "Microelectrokinetic turbulence in microfluidics at low Reynolds number". In: *Phys. Rev. E* 93.1 (2016), p. 013106. DOI: 10.1103/PhysRevE.93.013106.

[10] Martel M.J and Toner M. "Inertial Focusing in Microfluidics". In: *Annual Review of Biomedical Engineering.* 16 (2014), pp. 371–96.

[11] Laurell T and Lenshof A. "Lab exercise instruction – Acoustophoresis". In: (2016).

[12] Petersson F, Åberg Lena, Swärd-Nilsson Ann-Margret and Laurell T. "Free flow acoustophoresis: microfluidic-based mode of particle and cell separation". In: *Analytical Chemistry.* 79.14 (2007), pp. 5117–23. DOI: 10.1021/ac070444e.

[13] Krieghoff-Henning E, Folkerts J, Penzkofer A and Weg-Remers S. "Cancer – an overview". In: *Med Monatsschr Pharm.* 40.2 (2017). PMID: 29952494, pp. 48–54.

[14] Patel A. "Benign vs Malignant Tumors". In: *JAMA Oncology.* 6.9 (2020), p. 1488. DOI: 10.1001/jamaoncol.2020.2592.

[15] World Health Organization. *Cancer?* [Accessed: 05 22, 2023]. URL: {https://www.who.int/health-topics/cancer#tab=tab_1}.

[16] Undvall Anand E, Magnusson C, Lenshof A, Ceder Y, Lilja H and Laurell T. "Two-Step Acoustophoresis Separation of Live Tumor Cells from Whole Blood". In: *Analytical Chemistry.* 93.51 (2021), pp. 17076–17085. DOI: 10.1021/acs.analchem.1c04050.

[17] Leslie SW, Soon-Sutton TL, R I A and Siref LE. Sajjad H. "Prostate Cancer". In: *StatPearls [Internet]. Treasure Island (FL): StatPearls.* (2023). PMID: 29261872.

[18] Geltmeier A, Rinner B, Bade D, Meditz K, Witt R, Bicker U, Bludszuweit-Philipp C and Maier P. "Characterization of Dynamic Behaviour of MCF7 and MCF10A Cells in Ultrasonic Field Using Modal and Harmonic Analyses". In: *PLoS One.* 10.8 (2015). DOI: 10.1371/journal.pone.0134999.

[19] Uggeri J, Gatti R, Belletti S, Scandroglio R, Corradini R, Rotoli BM and Orlandini G. "Calcein-AM is a detector of intracellular oxidative activity". In: *Histochem Cell Biol.* 122.5 (2004), pp. 499–505. DOI: 10.1007/s00418-004-0712-y.

[20] Martin NC, Pirie AA, Ford LV, Callaghan CL, McTurk K, Lucy D and Scrimger DG. "The use of phosphate buffered saline for the recovery of cells and spermatozoa from swabs". In: *Sci Justice.* 46.3 (2006), pp. 179–84. DOI: 10.1016/S1355-0306(06)71591-X.

[21] Jang TH, Park SC, Yang JH, Kim JY, Seok JH, Park US, Choi CW, Lee SR and Han J. "Cryopreservation and its clinical applications". In: *Integr Med Res.* 6.1 (2017), pp. 12–18. DOI: 10.1016/j.imr.2016.12.001.

[22] McKinnon KM. "Flow Cytometry: An Overview." In: *Curr Protoc Immunol.* 120.5 (2018). DOI: 10.1002/cpim.40.

[23] Péroux L. "Pushing the boundaries of acoustic particleseparation: achieving high-throughput, avoidingspillover effects, investigating the effects of theparticle concentration, and measuring acousticproperties". In: (2022).

APPENDIX A

Figures from experiments - Polystyrene beads

Two figures taken at the outlet fork from each experiment made with polystyrene beads are presented - one in the beginning before the particles have separated, and one in the end when/if the particles have separated. In all figures, the flow goes from right to left.

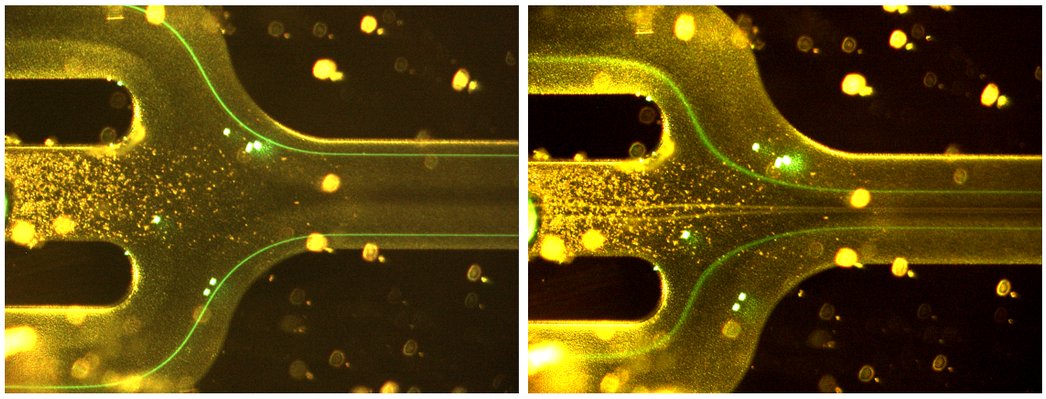

(a) (b)

Figure A.1.: Red 9.89 μm and green 5.19 μm polystyrene beads in MQ water. a) $r_{in} = 0.8$, $r_{out} = 0.2$. $Q_{tot} = 200$ μL/min. No separation is seen. b) $r_{in} = 0.8$, $r_{out} = 0.2$. $Q_{tot} = 200$ μL/min. Separation is seen

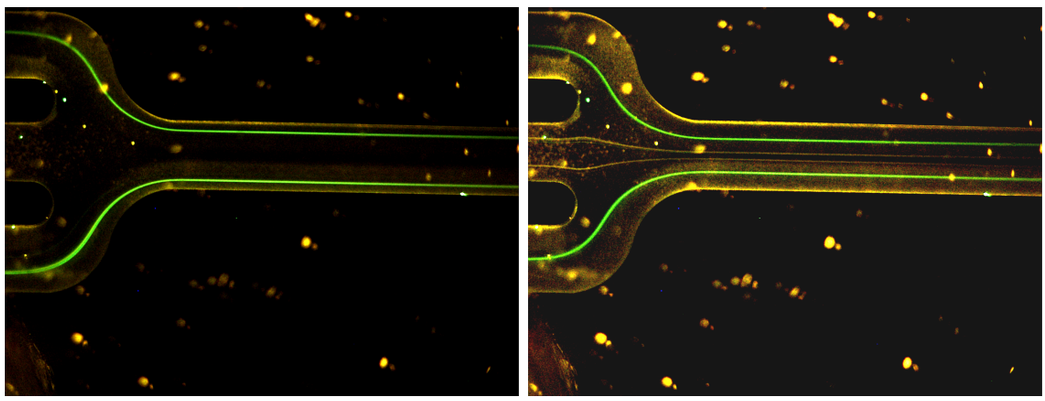

(a) (b)

Figure A.2.: Red 9.89 μm and green 5.19 μm polystyrene beads in 20% Iodixanol. Here, the picture is taken more zoomed out than other pictures taken. The reason to why a different magnification was used was because it was forgotten to change to the "correct" one after the chip was cleaned. a) $r_{in} = 0.8$, $r_{out} = 0.2$. $Q_{tot} = 200$ μL/min. No separation is seen. b) $r_{in} = 0.8$, $r_{out} = 0.2$. $Q_{tot} = 200$ μL/min. Separation is seen

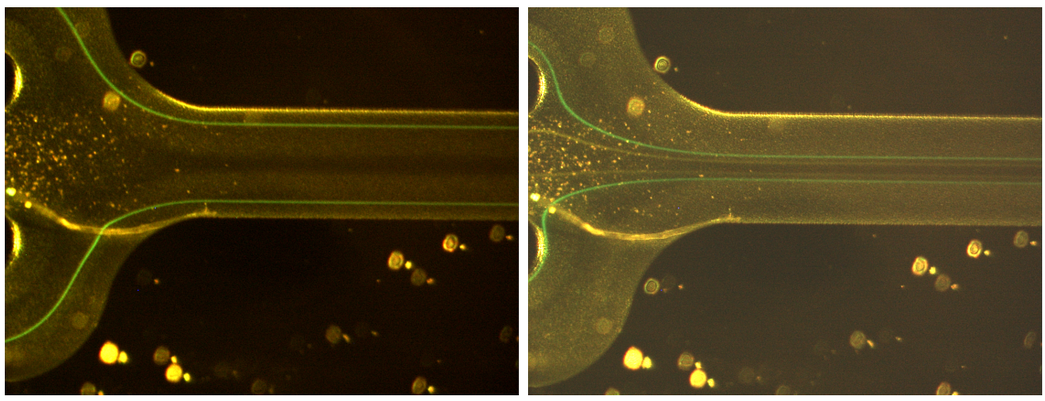

(a) (b)

Figure A.3.: Red 9.89 μm and green 7.81 μm polystyrene beads in MQ water. For this experiment, there was a fiber in the chip. However, this did not affect the separation as the fiber was far down in the chip. a) $r_{in} = 0.8$, $r_{out} = 0.2$. $Q_{tot} = 200$ μL/min. No separation is seen. b) $r_{in} = 0.8$, $r_{out} = 0.2$. $Q_{tot} = 200$ μL/min. Separation is seen

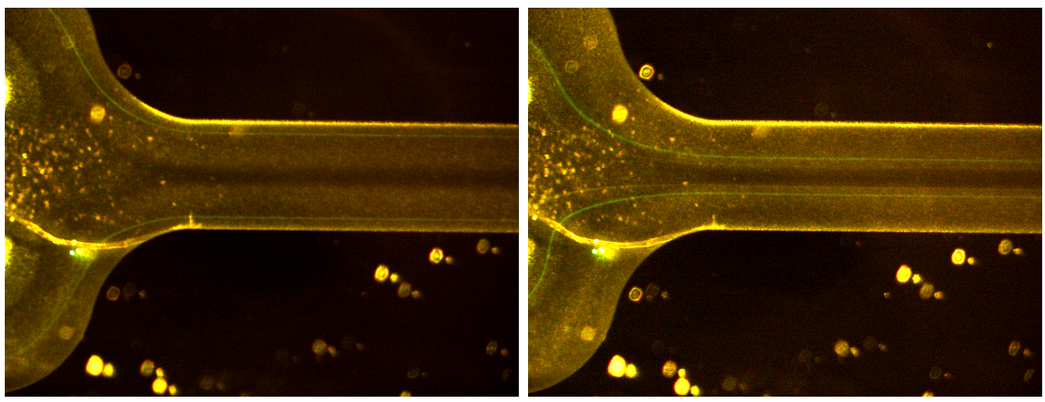

(a) (b)

Figure A.4.: Red 9.89 μm and green 7.81 μm polystyrene beads in 20% Iodixanol. For this experiment, there was a fiber in the chip. However, this did not affect the separation as the fiber was far down in the chip. Furthermore, the particles are very hard to see as there was a lot of problem with the set up during the experiment, hence the pictures are taken after the sample has been running for a while. a) $r_{in} = 0.8$, $r_{out} = 0.2$. $Q_{tot} = 200$ μL/min. No separation is seen. b) $r_{in} = 0.8$, $r_{out} = 0.2$. $Q_{tot} = 200$ μL/min. Separation is seen

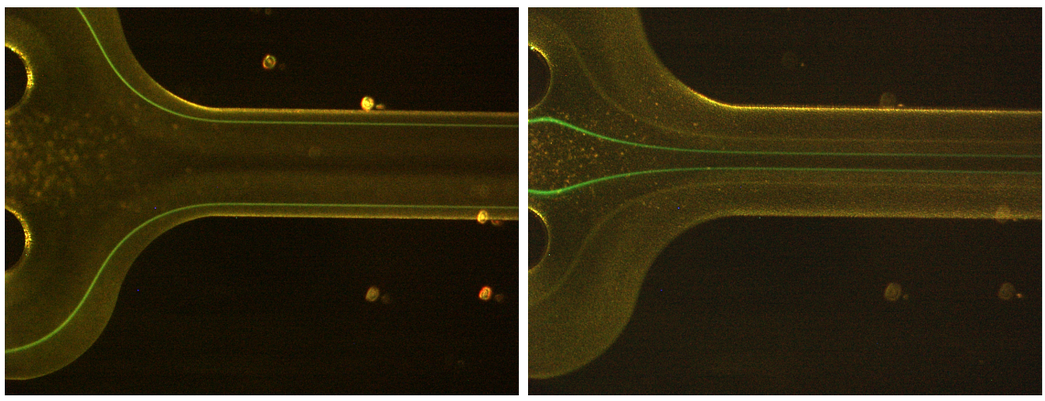

(a) (b)

Figure A.5.: Red 4.99 μm and green 7.81 μm polystyrene beads in MQ water. As the green particles are bigger, they move faster to the center, compared to the other two experiments. a) $r_{in} = 0.8$, $r_{out} = 0.2$. $Q_{tot} = 200$ μL/min. No separation is seen. b) $r_{in} = 0.8$, $r_{out} = 0.2$. $Q_{tot} = 200$ μL/min. Separation is seen

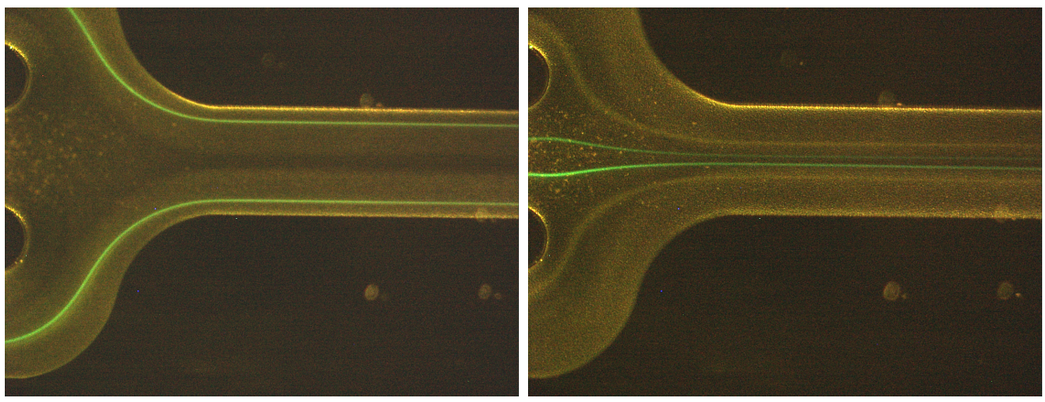

(a) (b)

Figure A.6.: Red 4.99 μm and green 7.81 μm polystyrene beads in 20% Iodixanol. As the green particles are bigger, the move faster to the center. a) $r_{in} = 0.8$, $r_{out} = 0.2$. $Q_{tot} = 200$ μL/min. No separation is seen. b) $r_{in} = 0.8$, $r_{out} = 0.2$. $Q_{tot} = 200$ μL/min. Separation is seen

APPENDIX B

Figures from experiments - DU145 cells

Two figures taken at the outlet fork from each experiment made with DU145 cells with polystyrene beads are presented - one in the beginning before the particles have separated from the cells, and one in the end when/if the particles have separated from the cells. In all figures, the flow goes from right to left.

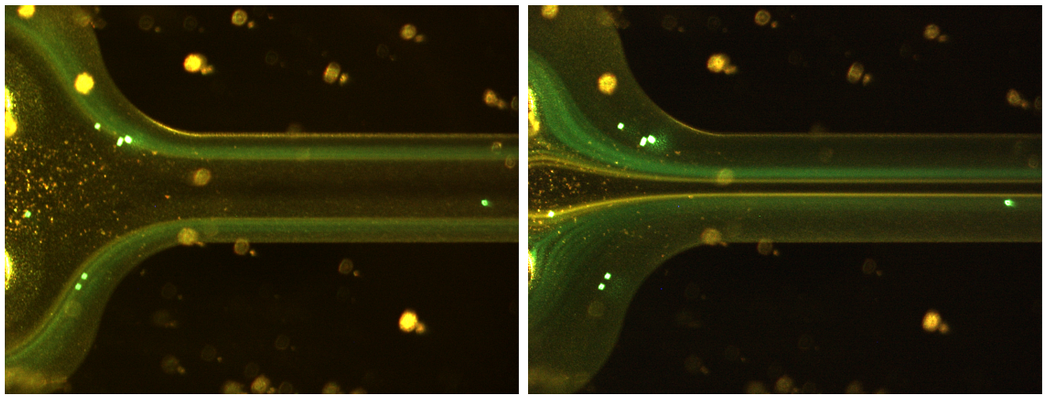

(a) (b)

Figure B.1.: DU145 cells with red 9.89μm polystyrene beads in PBS. a) $r_{in} = 0.8$, $r_{out} = 0.2$. $Q_{tot} = 50$ μL/min. No separation is seen. b) $r_{in} = 0.8$, $r_{out} = 0.2$. $Q_{tot} = 50$ μL/min. Separation is seen

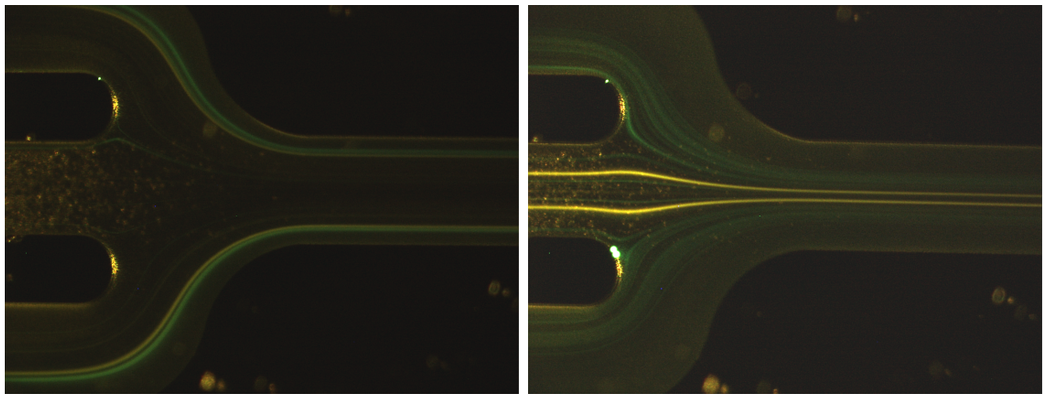

(a) (b)

Figure B.2.: DU145 cells with red 9.89μm polystyrene beads in 10% Iodixanol. a) $r_{in} = 0.8$, $r_{out} = 0.2$. $Q_{tot} = 50$ μL/min. No separation is seen. b) $r_{in} = 0.8$, $r_{out} = 0.2$. $Q_{tot} = 50$ μL/min. Separation is seen

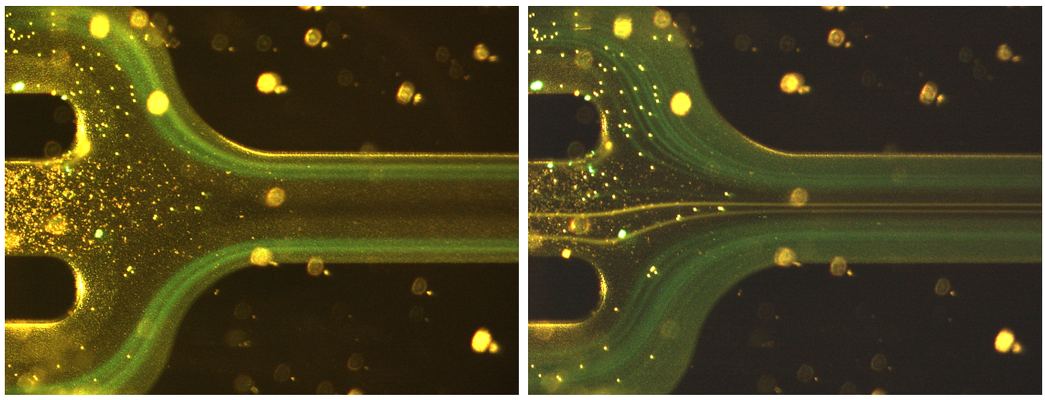

(a) (b)

Figure B.3.: DU145 cells with red 9.89μm polystyrene beads in 20% Iodixanol. a) $r_{in} = 0.8$, $r_{out} = 0.2$. $Q_{tot} = 50$ μL/min. No separation is seen. b) $r_{in} = 0.8$, $r_{out} = 0.2$. $Q_{tot} = 50$ μL/min. Separation is seen

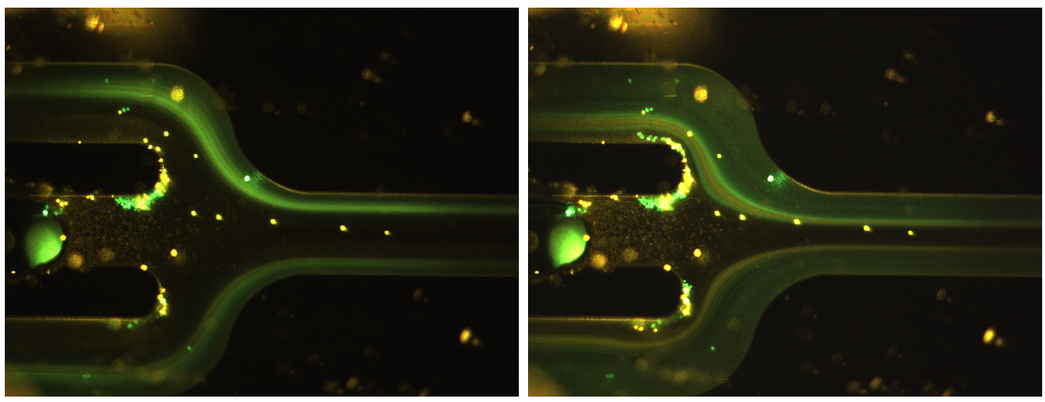

(a) (b)

Figure B.4.: DU145 cells with red 7.81μm polystyrene beads in PBS. a) $r_{in} = 0.8$, $r_{out} = 0.2$. $Q_{tot} = 50$ μL/min. No separation is seen. b) $r_{in} = 0.8$, $r_{out} = 0.2$. $Q_{tot} = 50$ μL/min. Separation is hard to see

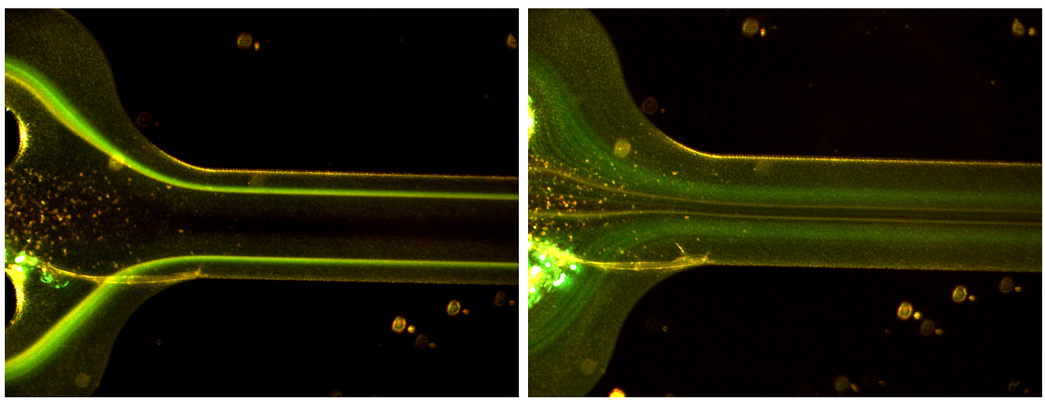

(a) (b)

Figure B.5.: DU145 cells with red 7.81μm polystyrene beads in 10% Iodixanol. For this experiment, there was a fiber in the chip. However, this did not affect the separation as the fiber was far down in the chip. Furthermore, this experiment was done the same day as the Red 9.89 μm and green 7.81 μm polystyrene beads in 20% Iodixanol. That experiment proved that the fiber did not affect the separation since the same result as another master student was given. a) $r_{in} = 0.8$, $r_{out} = 0.2$. $Q_{tot} = 50$ μL/min. No separation is seen. b) $r_{in} = 0.8$, $r_{out} = 0.2$. $Q_{tot} = 50$ μL/min. Separation is seen

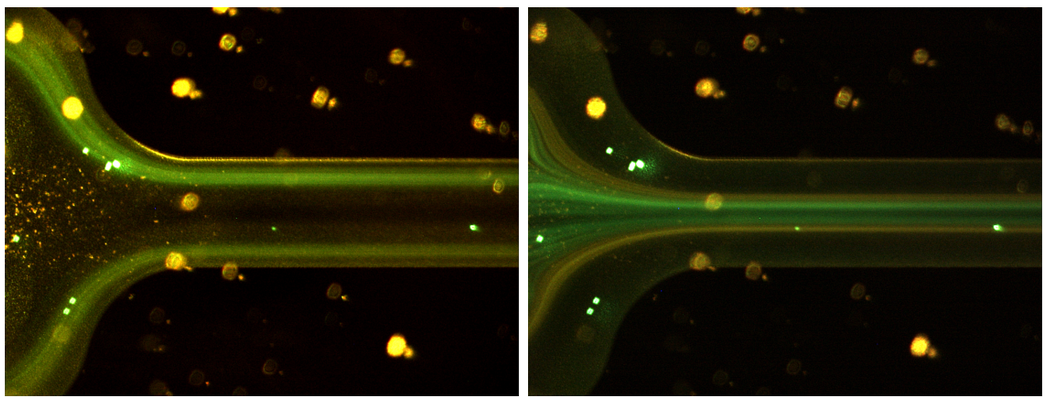

(a) (b)

Figure B.6.: DU145 cells with red 4.99μm polystyrene beads in PBS. a) $r_{in} = 0.8$, $r_{out} = 0.2$. $Q_{tot} = 50$ μL/min. No separation is seen. b) $r_{in} = 0.8$, $r_{out} = 0.2$. $Q_{tot} = 50$ μL/min. Separation is seen